

OBSERVED DYNAMIC TRAFFIC FEATURES ON A FREEWAY
SECTION WITH MERGES AND DIVERGES

by

SHAZIA MALIK

A research project report submitted in partial fulfillment
of the requirements for the degree of

MASTER OF SCIENCE
in
CIVIL AND ENVIRONMENTAL ENGINEERING

Portland State University

2003

PROJECT APPROVAL

The research project report of Shazia Malik for the Master of Science in Civil and Environmental Engineering submitted on July 30, 2003, is accepted by the faculty advisor and the department.

ADVISOR APPROVAL

Robert L. Bertini, Advisor

DEPARTMENT APPROVAL

Scott A. Wells, Chair
Department of Civil and Environmental Engineering

ACKNOWLEDGEMENTS

I wish to express my sincere appreciation to Professor Robert L. Bertini for supervising this research project. His guidance, patience and enthusiasm were invaluable.

I am indebted to Professor David Levinson and Lei Zhang of the University of Minnesota for generously providing the archived data and other site information used in this study.

A special thanks to the transportation research group at PSU: Monica Leal, Sutti Tantiyanugulchai, Roger Lindgren, Ahmed El-Geneidy and others. It was a privilege to work with them. They were always there to share their opinions, knowledge and helpful comments for which I am highly grateful. I am also indebted to Roger Lindgren for reviewing my work. His effort helped me in finalizing this project report. I would also like to thank Jenny Kincaid and Marianne Stupfel-Wallace for their help during my graduate studies.

Finally, my project would not have been possible without the support, love and patience of all my family members. In particular, I am grateful to my husband Haroon and my parents who have always been there for me. I owe my achievements to their continuous support and encouragement.

ABSTRACT

An abstract of the research project report of Shazia Malik for the Master of Science in Civil and Environmental Engineering submitted on July 30, 2003.

Title: Observed Dynamic Traffic Features On a Freeway Section With Merges And Diverges.

Traffic data measured on a two-lane freeway and its on-ramps (with metered flows) and off-ramps were carefully studied for four days during the rush hour. Certain features could be reproduced from day to day. A bottleneck arose consistently on all four days due to traffic merging and diverging at a freeway location. Detailed analysis during these times showed that queuing actually arose some distance downstream of a merge that also resulted in flow reductions measured at a downstream off-ramp. The queues were caused by drivers who had just entered the freeway's shoulder lane from the on-ramp and had slowed down to merge. The slowing of vehicles spread to both lanes and propagated upstream. The average discharge flows that accompanied the onset of queuing were found to be 4% lower than flows measured just prior to the queue's formation.

Upon bottleneck activation, flow reductions accompanied by increases in measured occupancies occurred sequentially in time and space marking the passage of the backward-moving shock. Mean shock velocities ranged from 20 to 24 mph (32 to 40 km/h). Oscillations arose in the queue and propagated upstream from the bottleneck at nearly constant speeds. The effects of these oscillations were not felt downstream of the bottleneck. The analysis used transformed curves of cumulative vehicle counts and cumulative occupancy to obtain the measurement resolution necessary for studying important traffic features. The site is located in Minneapolis, Minnesota, USA, and data were collected prior to a ramp meter shut down experiment conducted by the Minnesota Department of Transportation (Mn/DOT) in 2000.

TABLE OF CONTENTS

1. INTRODUCTION	1
2. METHODOLOGY	2
2.1. Background.....	3
2.2. Diagnostic Tools.....	4
3. DATA	10
4. OBSERVATIONS	16
4.1. Day One.....	16
4.1.1. Day One: Bottleneck and Queue Detection.....	18
4.1.2. Day One: Bottleneck Discharge Flows.....	24
4.1.3. Day One: Ramp Analysis.....	25
4.1.4. Day One: Shock Characteristics.....	28
4.1.5. Day One: Traffic Oscillations.....	29
4.2. Reproducing the Observations.....	31
4.2.1 Reproducible Bottleneck Features	32
4.2.2. Variation in Shock Propagations.....	33
5. CONCLUSIONS	34
REFERENCES	37
APPENDIX A: Climatological Data	39
APPENDIX B: Details of Shock Variations by Day	40

LIST OF TABLES

Table	Title	Page
1	Off-Ramp Magnitudes (March 20, 2000; From 17:00 to 18:00).....	13
2	Shock Velocity Variations.....	28
3	Summary of Measured Traffic Features.....	33
4	Four Days: Shock Characteristics.....	34
5	Day 1 – Shock Propagation.....	40
6	Day 2 – Shock Propagation.....	40
7	Day 3 – Shock Propagation.....	40
8	Day 4 – Shock Propagation.....	41

LIST OF FIGURES

Figure	Title	Page
1	Time-Space Diagram for Congested Traffic.....	4
2	Input-Output Diagram.....	5
3	Queuing Diagram.....	7
4	Cumulative Vehicle Counts ($N(x, t)$) for a Freeway Location.....	8
5	Oblique $N(x, t)$ for a Freeway Location.....	9
6	Oblique $T(x, t)$ for a Freeway Location.....	10
7	Site Map – US 169.....	11
8	Volume Adjustment Example.....	14
9	Oblique $N(x, t)$ and $T(x, t)$ Downstream of Bottleneck (Station 18) ..	15
10	Day One: Raw Occupancy Data for Station 16.....	16
11	Day One: Occupancy Contour Map.....	17
12	Day One: Transformed $N(x, t)$	19
13	Day One: Oblique $N(x, t)$ and $T(x, t)$	20
14	Day One: Oblique $N(x, t)$ and $T(x, t)$ Per Lane (a) Station 13; (b) Station 14; (c) Station 15; (d) Station 16.....	22
15	Day One: Transformed $N(x, t)$ Showing End of Queue between Stations 12 and 18.....	23
16	Day One: Oblique $N(x, t)$ and $T(x, t)$ at Station 18.....	25
17	Oblique $N(x, t)$ Showing Ramp Flows between Stations 16 and 17.....	26
18	Aerial Photo of US 169 and TH-55 Interchange.....	27
19	Day One: Deviations from the Prevailing Flows ($N-N_{I0}$).....	30
20	Oblique $N(x, t)$ Showing Ramp Flows between Stations 16 and 17 (Day Three).....	32

1. INTRODUCTION

This empirical analysis describes queue features at a freeway bottleneck that became active due to traffic merging and diverging. It is shown that the bottleneck became active during the evening rush hour immediately after the influx of traffic rose on an on-ramp. This was accompanied by a sudden drop in the exiting ramp flow downstream of the on-ramp indicating that queuing arose between the on- and the off-ramps. This queuing was apparently caused by drivers who had just entered the freeway at reduced speeds in order to negotiate discretionary lane-change maneuvers. The flow in the shoulder lane at these times was quite high since the exit was located 0.1 mile (0.16 km) downstream of the merge.

From this study, certain reproducible patterns were observed. For example, the location of the bottleneck and the patterns of flow observed on the ramps in its vicinity were consistent for all days of analysis. The average discharge flow measured after the bottleneck became active also did not vary much from day to day. The onset of queuing was marked by a sudden drop in flow and rise in measured occupancy. The velocity of the backward-moving shock marking the onset of queuing was also similar from day to day. Forward-moving waves of lower flows were also observed to travel at reproducible velocities. The start-stop waves (or oscillations) observed in congested freeway traffic propagated upstream, against the flow of the traffic. These oscillations were flow changes that appeared as stop-and-go driving conditions to motorists traveling along the congested route (Mauch, 2002). The amplitude of the flow above the average flow that prevailed at a specific time at each upstream location did not grow with distance from the head of the queue. The flow at the downstream locations remained smooth.

Some of the observations made in this study remain consistent with earlier empirical studies of freeway bottlenecks. The study is unique in that it applies a methodology that

requires conservation of vehicles over space and time to a heterogeneous site where each freeway detector station is preceded by at least one on-ramp and one off-ramp. This study used cumulative vehicle arrival curves and cumulative curves of vehicle occupancy measured at neighboring loop detectors, transformed in ways that reveal traffic characteristics of interest. A detailed description of the methods used is presented in section 2. Subsequently, section 3 describes the freeway site, data that were collected and adjustments that were necessary to ensure that consecutive stations counted the same total number of vehicles. This enabled construction of cumulative vehicle arrival curves across merges and diverges that helped identify the bottleneck's location and the times it remained active. Earlier studies on traffic flow have used similar procedures for studying merges (Bertini, 1999; Bertini and Cassidy, 2002; Cassidy and Bertini, 1999a; Cassidy and Bertini, 1999b; Cassidy and Mauch, 2001; Windover and Cassidy, 2001) and diverges (Munoz and Daganzo, 2000).

Section 4 presents the observations. Making use of at least five successive detector stations (three upstream and two downstream of the bottleneck), the analysis includes identification of the bottleneck's location and time it remained active, along with bottleneck discharge features, merging and diverging ramp flow analyses, wave propagation upon queue formation and flow oscillations that occurred in congested traffic. Some findings from repeating these analyses with data from other days are also included. Finally, section 5 provides some concluding remarks.

2. METHODOLOGY

This section briefly discusses the background of the empirical analysis of traffic flow phenomena. This is followed by a description of the diagnostic tools used herein – transformed

curves of cumulative vehicle arrival number and measured occupancy. The use of these tools provided the resolution necessary to reveal details of the traffic stream.

2.1 Background

Traffic studies based on kinematic wave theory show that in uncongested traffic, changes in flow due to sustained changes in demand propagate downstream. In congested traffic, changes in flow propagate upstream and there is an interface that separates the two states (May, 1990; Windover, 1998; Windover and Cassidy, 2001). These are indicated as states I and II in the sample time-space diagram shown in Figure 1. The conventional approach for determining the time and distance in a queue uses a time-space diagram to examine vehicle trajectories (Lawson et al., 1997). Figure 1 shows a hypothetical flow of vehicles from x_1 to x_3 for a homogeneous highway section with a bottleneck located at x_2 . An active bottleneck is a location on the network, downstream of which exist free-flow conditions and upstream of which is a queue (Daganzo, 1997). On a homogeneous highway, a bottleneck can become active once the demand at that section exceeds capacity. There are more vehicles at t_1 that want to be served than are capable of being served by the system (May, 1990).

State III is the phase past the bottleneck where vehicles, after having passed through the queued conditions in state II, accelerate to higher speeds that are insensitive to flow. If a stationary observer were to view an arbitrarily designated vehicle (reference vehicle) v_1 , each vehicle of higher arrival number would follow the motion of v_1 in the same state. Vehicles in each state maintain a headway, spacing, and velocity common to all other vehicles. Although the actual bottleneck lies at x_2 , drivers traveling between x_1 and x_2 (marked by the backward-moving shock w_1) feel its impact without actually knowing what caused them to slow down. This backward-moving shock between the upstream free-flow state I and the queued state II

shows the location of the back of the queue as a function of time, t . At every point along the back-of-queue trajectory, the slope is the instantaneous speed at which the back of the queue is moving along the highway. This speed (V_i) is related to the change in flow (Δq) and change in density (Δk) across the interface, by the well-known relationship $V_i = \Delta q / \Delta k$ (Lawson et al., 1997). This relationship forms the basis of the kinematic wave theory of traffic flow. For Figure 1, it is assumed that data on volume, occupancy and arrival time of vehicles are available at locations x_1 , x_2 and x_3 .

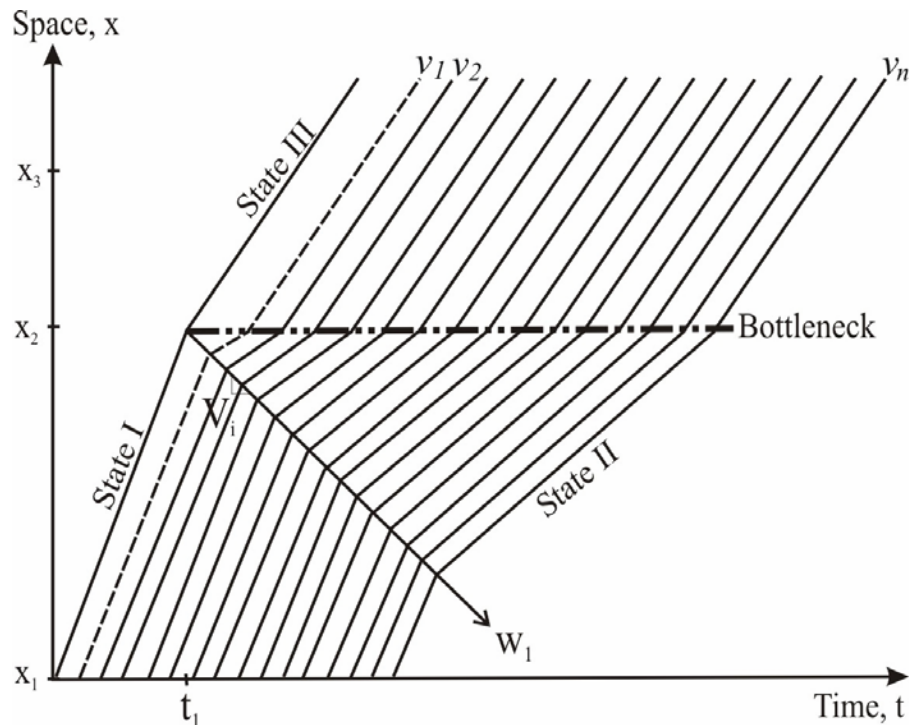


Figure 1: Time-Space Diagram for Congested Traffic

2.2 Diagnostic Tools

Newell (1993) used assumptions about wave motion to predict the features of cumulative vehicle arrival curves. Thus, an input-output diagram, as shown in Figure 2, could be used to determine the number of vehicles in a homogeneous highway section at a particular

time, and vehicular trip times. Figure 2 presents hypothetical cumulative curves of vehicle arrival number passing location x_i by time t . $N(x_1, t)$ and $N(x_2, t)$ are curves constructed for two locations x_1 and x_2 , measured from the passage of some reference vehicle, i ; i.e., both curves describe the same collection of vehicles. The vertical distance between the curves at some time, t_1 , is the number of vehicles between locations x_1 and x_2 . Also, the horizontal distance for some vehicle j is the vehicular trip time between x_1 and x_2 . Thus, the slope of $N(x_i, t)$ at any time is the flow corresponding to the total number of vehicles that passed the location x_i by time t .

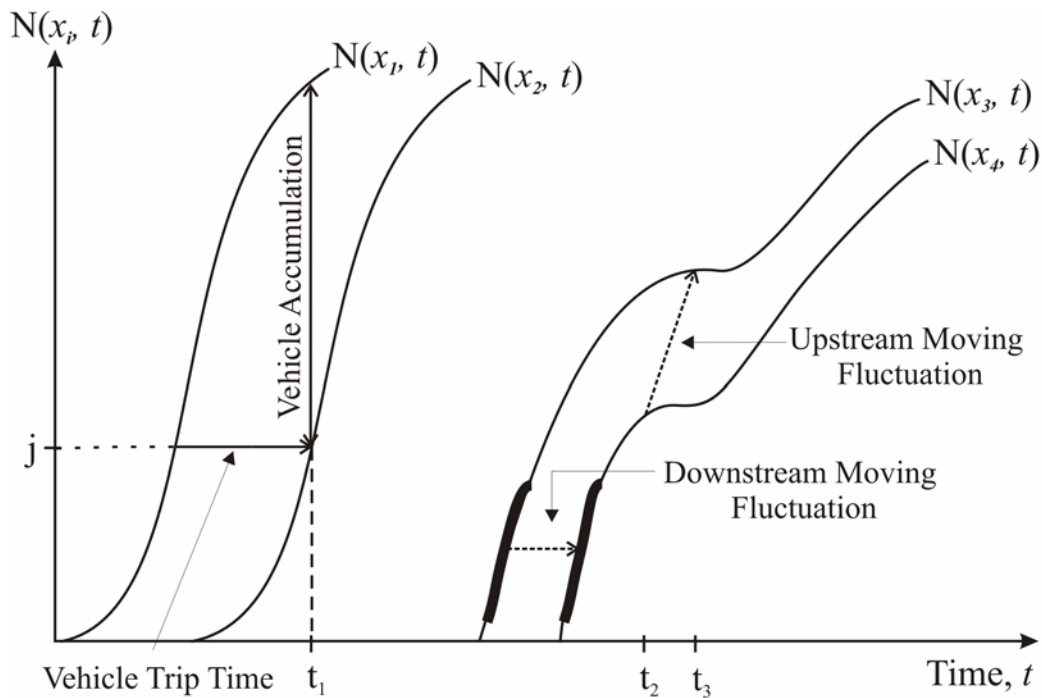


Figure 2: Input-Output Diagram

The propagation of changing traffic conditions can be observed from these $N(x, t)$. Figure 2 also shows two other curves, $N(x_3, t)$ and $N(x_4, t)$, that describe vehicles traveling during a peak period from x_3 towards x_4 . Time t_2 marks the onset of congestion. As seen in the figure, any fluctuation in flow on curve $N(x_3, t)$ before t_2 is passed horizontally to the

downstream curve $N(x_4, t)$ among the same collection of vehicles (Windover, 1998). This replication across $N(x, t)$ is no longer horizontal when vehicles enter congestion from a free-flowing traffic state (seen as state I to II in Figure 1). The congested state results in vehicle decelerations that propagate upstream, opposite to the direction of flow. As congestion sets in around time t_2 , there is a drop in flow at x_4 that results in a non-horizontal upstream-moving wave arriving at x_3 at a later time t_3 . The upstream-moving fluctuation marks the arrival of the tail of the queue at x_3 accompanied by a drop in flow at time t_3 . The upstream-moving fluctuation can have a velocity that may depend on the driver characteristics and area type.

To further evaluate queue features, Figure 3 shows a queuing diagram constructed by shifting the upstream $N(x_1, t)$ to the right by the free flow travel time between x_1 and x_2 (Newell, 1982; Newell, 1993). If vehicles are conserved between x_1 and x_2 , superimposed $N(x, t)$ show that traffic was free flowing between the two stations. Any vertical separations between $N(x_1, t)$ and $N(x_2, t)$ in Figure 3 show the excess vehicle accumulation and the horizontal separation is the excess travel time, or delay.

As will be described in section 3, this study used vehicle count data provided by inductive loop detectors. Loop detectors can also provide occupancy data. Occupancy, represented here by T , is measured in units of total time spent by vehicles atop the detectors by time t (Cassidy et al., 2002). If measured occupancies were plotted cumulatively in the same manner as vehicle number for x_3 and x_4 in Figure 2, one would observe a sudden rise in occupancy at t_2 at x_4 , followed by rise in occupancy at t_3 at x_3 (Cassidy and Bertini, 1999b).

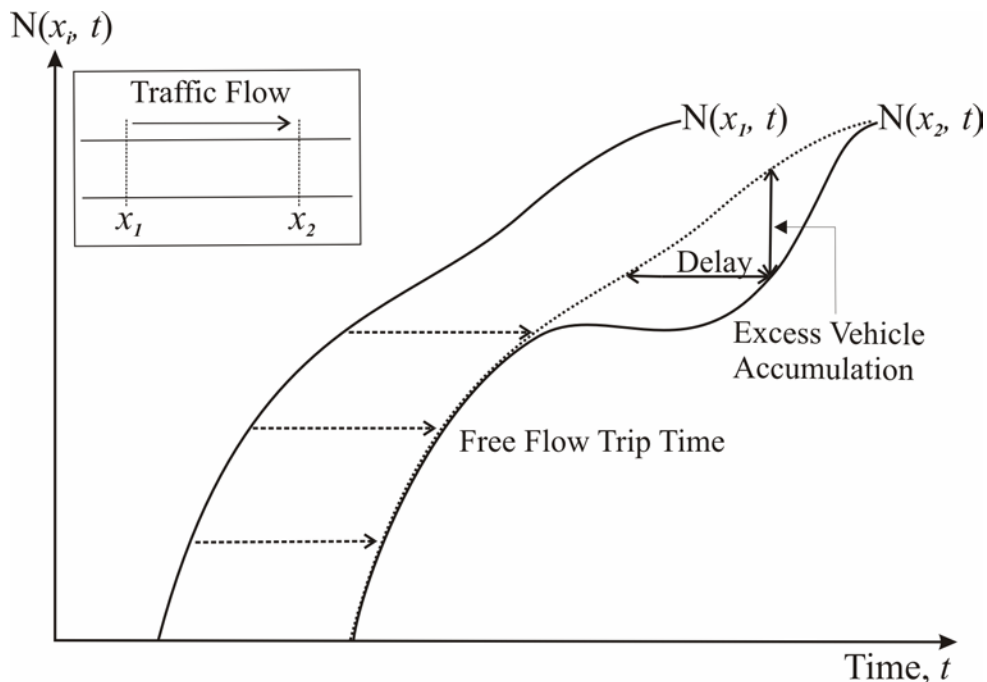


Figure 3: Queuing Diagram

The hypothetical $N(x, t)$ shown in Figures 2 and 3 clearly show the changes in flow. However, curves constructed from actual freeway count data over extended periods do not reveal flow changes in detail. One such curve plotted from the data used in this study is shown in Figure 4. An unaltered $N(x, t)$ would be a step function. To create smoothed $N(x, t)$, piecewise linear interpolations through the near-side top of each step were used. The cumulative vehicle count has been taken for over two hours as measured across two freeway lanes. Clearly, it is difficult to discern the details of flow changes.

Details of traffic flow can be magnified by using an oblique coordinate system where $N(x, t)$ is reduced by $q_o(t - t_o)$, with a rescaling rate q_o and t_o as the curve's starting time. Figure 5 shows an oblique plot using the same data as in Figure 4. The value of q_o was chosen by iteration so that the range of $N - q_o(t - t_o)$ was small as compared to the N itself and provided the best visualization for traffic features such as increases and decreases in flow. This method is

identical to that described in Bertini (1999), Bertini and Cassidy (2002); Cassidy and Bertini (1999), Cassidy and Bertini (1999a), Cassidy and Bertini (1999b), Cassidy and Mauch (2001), Cassidy and Windover (1995), and Munoz and Daganzo (2000).

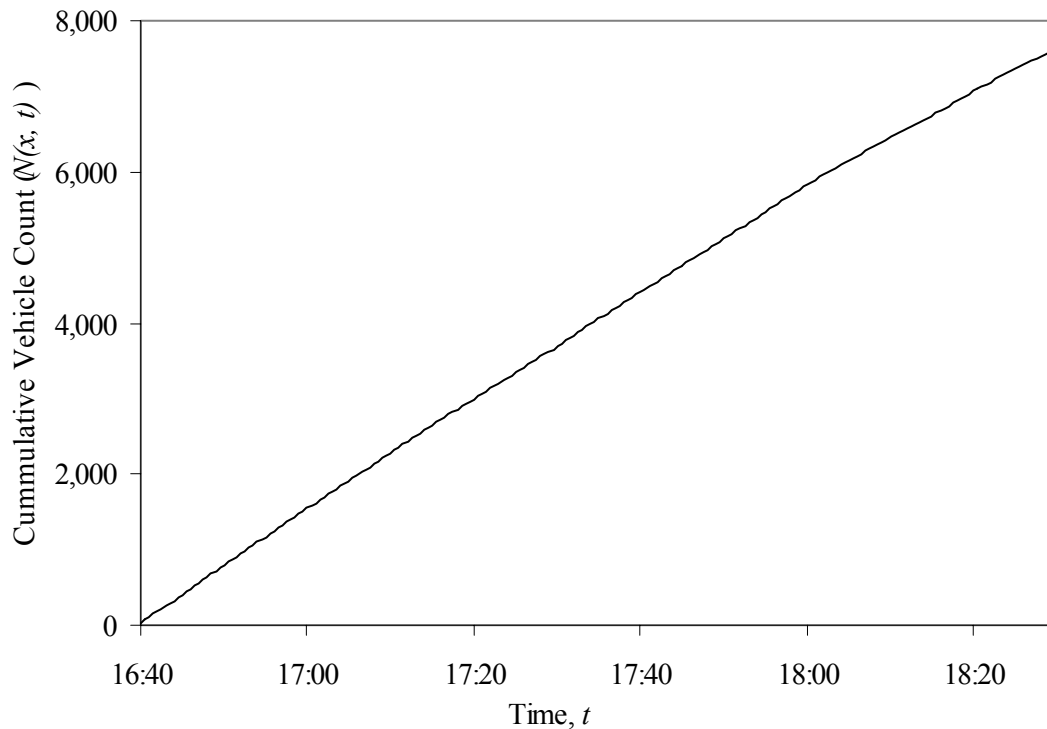


Figure 4: Cumulative Vehicle Count ($N(x, t)$) for a Freeway Location

Comparing Figures 4 and 5, the curve features appear magnified in the latter, making it possible to identify three notable flow changes at t_1 , t_2 and t_3 that were not visible in Figure 4. The flow changes are marked on the oblique $N(x, t)$ by piecewise linear approximations made by eye (marked by dashed lines). Thus, periods of nearly constant average flow are visually identified on Figure 5, shown in units of vehicles per hour (vph).

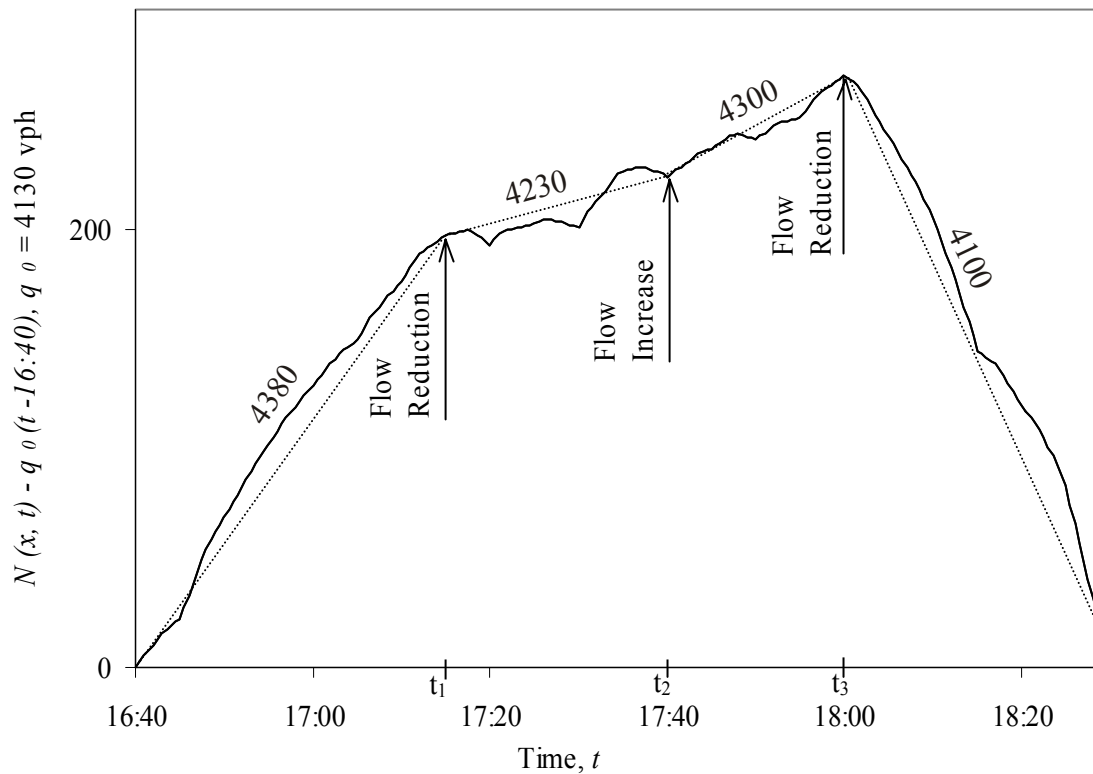


Figure 5: Oblique $N(x, t)$ for a Freeway Location

Curves of measured cumulative occupancies can be used to verify traffic features observed from oblique $N(x, t)$. $T(x, t)$ is the cumulative occupancy measured at station x by time t . Piecewise linear approximations to $T(x, t)$ were constructed as shown in Figure 6 for the same location and time used in Figures 4 and 5. An oblique coordinate system was also used following the same methodology described above. $T(x, t)$ was reduced by $b_o(t - t_o)$, where b_o is a rescaling rate while t_o is the curve's starting time. The oblique $T(x, t)$ improve the resolution of occupancy features at location x . Since the location considered in these figures was downstream of a bottleneck, Figure 6 shows oblique $T(x, t)$ following a similar pattern as the oblique $N(x, t)$ in Figure 5. The three times t_1 , t_2 and t_3 are shown along with periods of nearly

constant occupancies (in units of seconds per hour (sec/h)). Further discussion of these plots is provided in section 4 of this report.

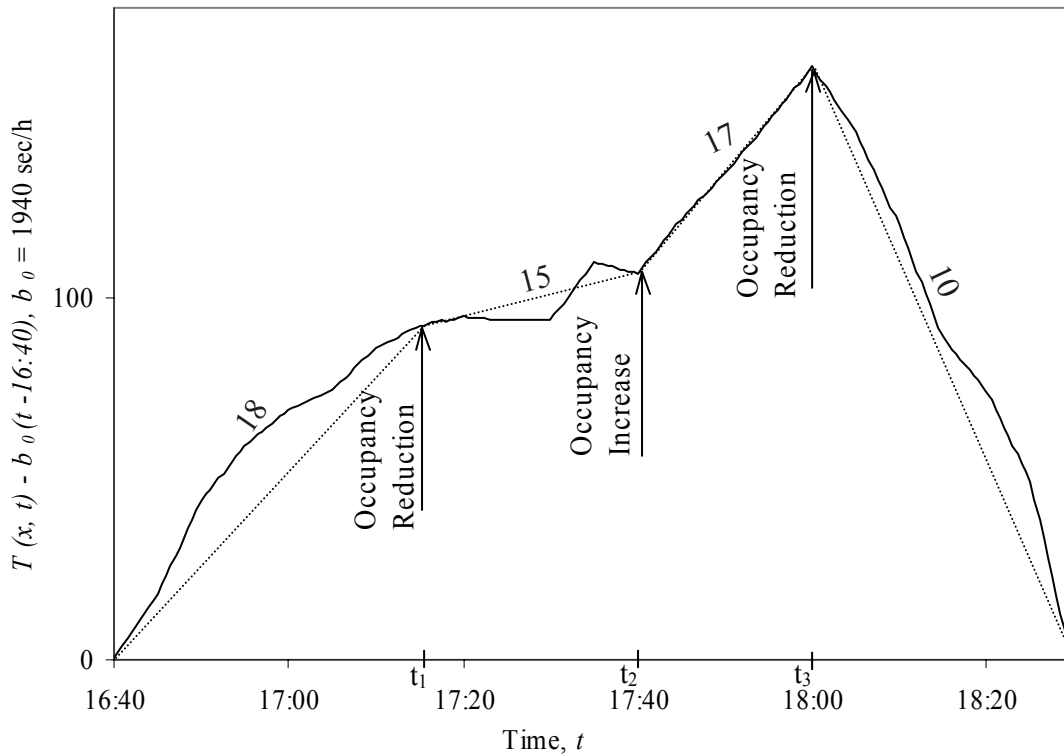


Figure 6: Oblique $T(x, t)$ for a Freeway Location

3. DATA

The traffic data analyzed in this study is from northbound highway US 169 located in Minneapolis, Minnesota. US 169 is a limited access freeway with ramp control. The traffic is characterized by high afternoon peak period flows. While the total length of the highway is approximately 16 miles (26 km) between I-494 and I-94, a 3-mile (4.8 km) section was chosen for this study. The site map is shown in Figure 7. This site was chosen due to the concentration of congestion between mileposts 128.8 and 131.7 for all days of analysis.

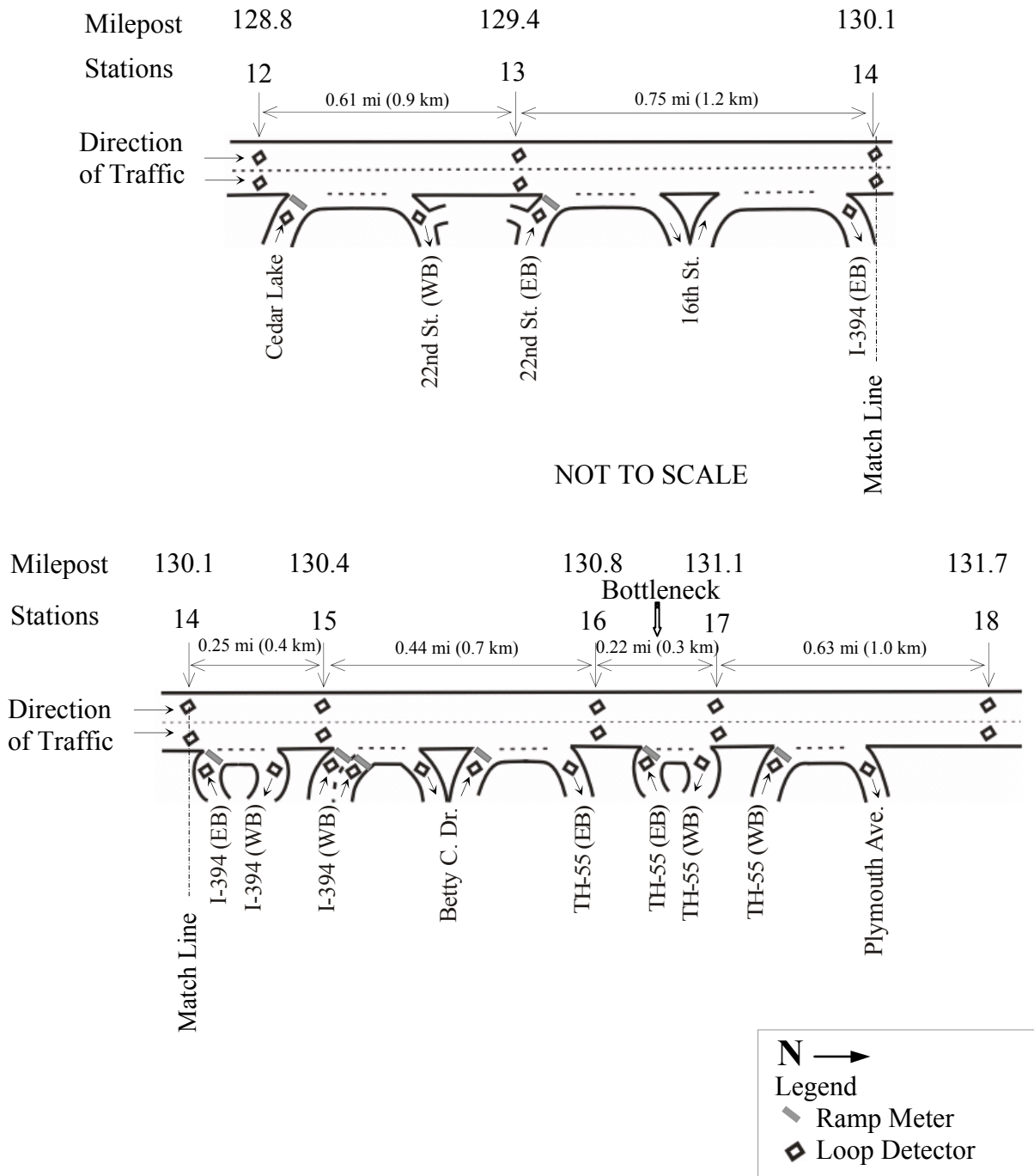


Figure 7: Site Map – US 169

Figure 7 shows that there were eight on- and eight off-ramps in the section of interest. The inductive loop detectors are shown as small diamonds in this figure. For the purpose of this

study, the loop detector stations were numbered 12 to 18 as shown. There were seven mainline detector locations with one detector located in each travel lane at each station. Both on- and off-ramps had detectors, except at the 16th St. interchange between stations 13 and 14. The posted freeway speed limit was 55 mph (88 km/h).

The loop detector data consisted of vehicle counts and detector occupancies (a dimensionless measure of density) measured over 30-second intervals. The data were available for four weekdays between 20 and 23 March, 2000. The conditions on this section of freeway were suitable for studying queue characteristics since the section consisted of two lanes with no lane drops and no obvious inhomogeneities other than the ramps and auxiliary lanes. There were no major incidents during the time periods analyzed. US 169 is a vital corridor that connects the City of Minneapolis to southwest Minnesota's manufacturing and agricultural centers and carries both commuter traffic as well as heavy commercial and recreational traffic. Two main highways, I-394 and Trunk Highway 55 (TH-55), also intersect US 169 between mileposts 130.1-130.4 and 130.8-131.1, respectively in the study area. As will be demonstrated in section 4, the bottleneck consistently formed between stations 16 and 17 on each of several afternoons studied. The weather conditions for all days considered for analysis were sunny except for March 23, 2000 when light rainfall was experienced. Appendix A contains weather conditions data for the city of Minneapolis, Minnesota, on days that were analyzed.

The $N(x, t)$ and $T(x, t)$ at each station described the measurements across both travel lanes. For the construction of $N(x, t)$ for stations 12 through 18, on- and off-ramp counts were included so that pairs of curves (discussed under section 4.1.1) described the same collection of vehicles during the study period. A pair-wise approach was adopted where the interchanges were modeled as single points along the freeway, including on-ramps and off-ramps located at

these points. Thus, cumulative vehicles measured upstream should equal those measured at the neighboring downstream station minus the interchange's net inflow. This suggestion was originally made by Newell (1993) and has been applied by several studies (Cassidy and Bertini, 1999a; Cassidy and Bertini, 1999b; Cassidy and Mauch, 2001; Windover and Cassidy, 2001.)

Using this methodology for the site selected, results from station pairs showed that the upstream volume minus the interchange's net inflow did not exactly equal the neighboring downstream volume. During uncongested periods, the vehicle counts for the analysis period indicated a loss of vehicles when comparing the upstream and the downstream stations. None of the detectors appeared to be malfunctioning at any time. Therefore, the reason for the loss was inferred to be that the off-ramp detectors were missing vehicles. This kind of behavior by exiting traffic is sometimes observed where, due to the wide gore area, vehicles do not pass over the ramp detectors but rather go around them. It is recognized that the study would have benefited from video data for the site. In the absence of such data, minor adjustments were made to the exiting ramp flows in order to maintain vehicle conservation between each pair of neighboring stations. Table 1 shows five off-ramp volumes for March 20, 2000, adjusted between 17:00 and 18:00. The volume changes ranged from 4 to 38 vph, or 3 to 11% and were of similar magnitudes for all days analyzed. Adjustments were applied primarily at the

Table 1: Off-Ramp Magnitudes (March 20, 2000; From 17:00 to 18:00)

Stations	Exit Ramp Volume (vph)			Net Change (%)
	Data	Adjusted	Difference	
12-13	38	42	4	11
14-15	441	454	13	3
15-16	459	497	38	8
16-17	293	305	12	4
17-18	141	149	8	6

beginning and end of the study periods when unqueued conditions persisted. Also, these adjustments were made to upstream flows after studying the $N(x, t)$ and $T(x, t)$ for each pair of stations.

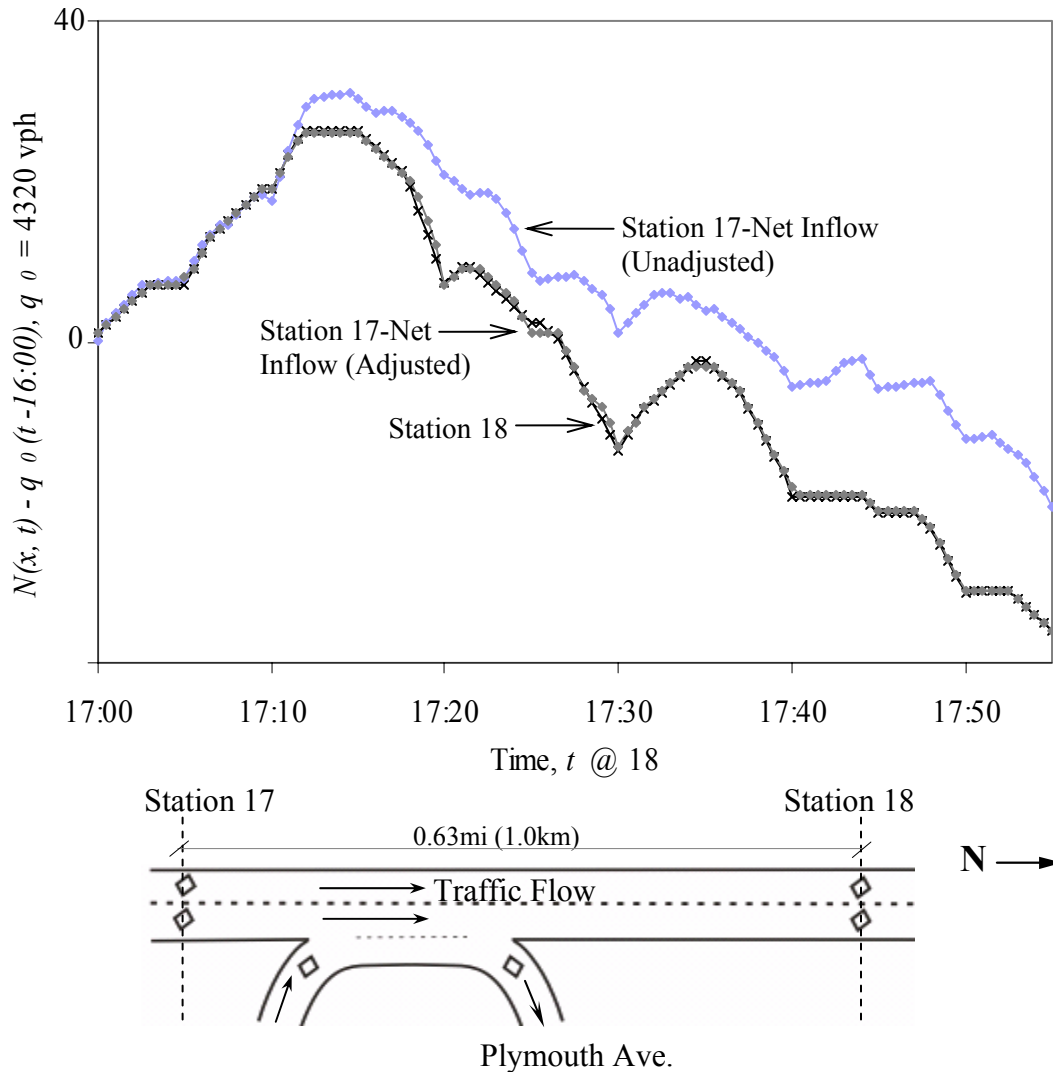


Figure 8: Volume Adjustment Example

An example of this procedure is shown in Figure 8 that was plotted for station 17 (minus net inflow) and 18 for March 20, 2000. A schematic sketch of the two stations is also shown below the plot. As seen in Figure 8, the traffic between the stations had nearly-stationary

characteristics where the fluctuations in flow at station 17 (minus net inflow) were seen at station 18 a short time later taking in consideration the free-flow vehicle trip time. This could have resulted from two traffic states; when the traffic was freely flowing or when it had already entered congestion (Cassidy, 1998). Oblique $T(x, t)$ and $N(x, t)$, shown in Figure 9¹ confirmed that the queue was not present at this location since the curves do not display any abrupt reduction in $N(x, t)$ accompanied by a rise in $T(x, t)$, a feature that would mark the arrival of a queue from downstream. Both curves display very similar features, indicating that the stationary traffic state that existed between stations 17 and 18 was free-flow. The vehicle accumulations that appear between the stations are actually due to the off-ramp, prior to station 18, under-counting the number of vehicles leaving the system. In this case an adjustment of 8 vph, or 6% of the off-ramp volume, corrected the problem. Such adjustments do not effect

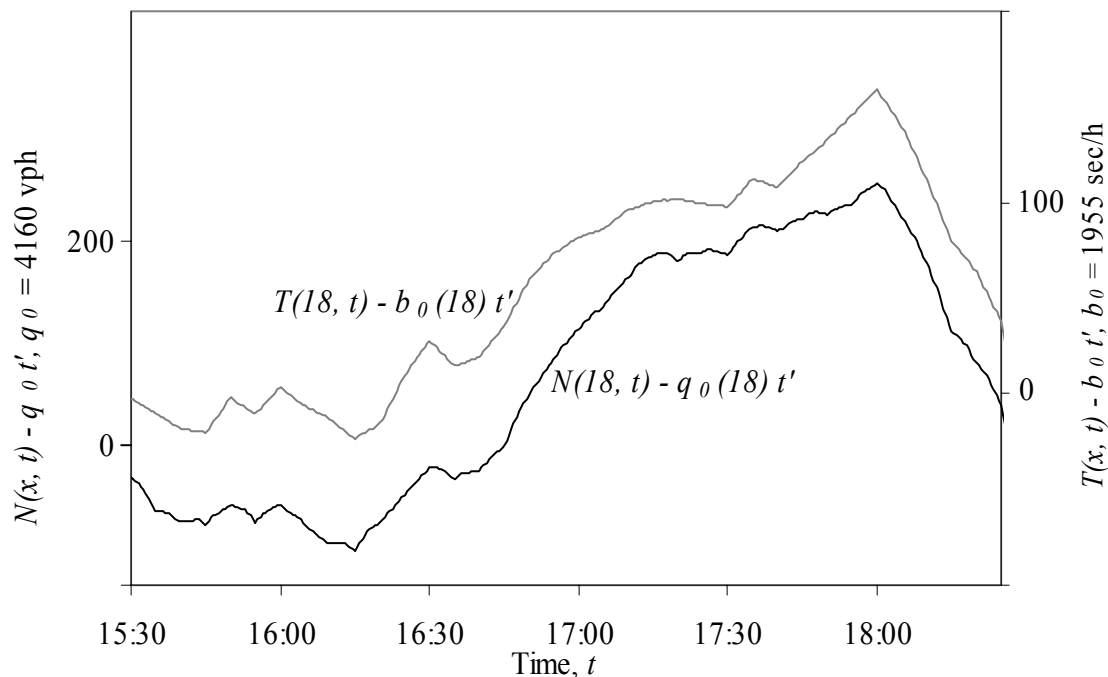


Figure 9: Oblique $N(x, t)$ and $T(x, t)$ Downstream of Bottleneck (Station 18)

¹ The time period, t' , is defined as $t - t_0$.

vehicle or wave trip times, but should be taken into account when evaluating vehicular accumulations between stations. The effects of corrected counts also did not influence the analyses.

It should be noted that during the evening peak periods analyzed for this study, all on-ramps were metered.

4. OBSERVATIONS

4.1 Day One

The day of analysis was Monday, March 20, 2000. The local weather service showed that it was a dry day. The analysis began by plotting raw occupancy data for 24 hours for all detector stations on US 169. Figure 10 shows an example of such a plot for station 16. This helped to identify the peak period and the stations where the study should concentrate for analysis. As seen in Figure 10, the peak period occurred between 17:00 and 18:00 where the occupancies suddenly rose to form a peak.

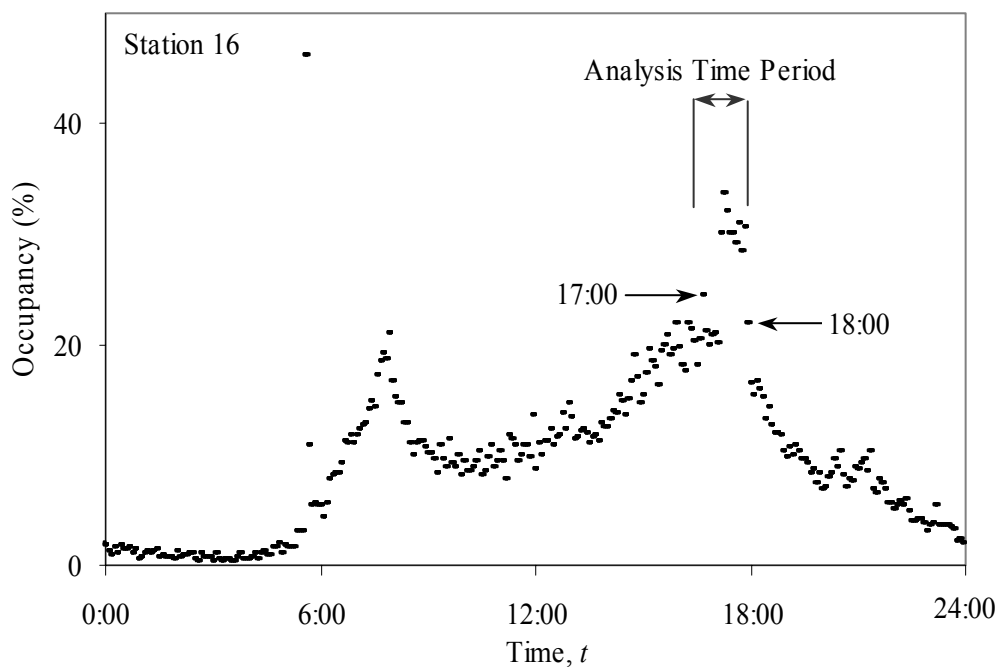


Figure 10: Day One: Raw Occupancy Data for Station 16

In order to verify the extent of congestion and the likely location of the bottleneck, a raw occupancy contour plot, as shown in Figure 11, was also constructed. In Figure 11, the y-axis is the station location, the x-axis is the time period, and the color variation represents occupancy, from green for lower occupancy to blue for higher occupancy. From the figure, it appeared that a bottleneck occurred in the vicinity of stations 16 and 17. Lower occupancy (an indication of higher speeds since it is a surrogate of density) occurred at station 17 and 18 during the whole day except at 16:45 at station 17 when the occupancy suddenly rose to 50%. This may have been a minor incident that lasted around 10 minutes and ended before 17:00. Since occupancy values of more than 28% are an indication of congested conditions (May, 1990), Figure 11 shows that congestion propagated over several miles upstream of station 16 and began to dissipate beginning at station 12. The minor incident that occurred between stations 17 and 18 had no impact on the traffic conditions observed later.

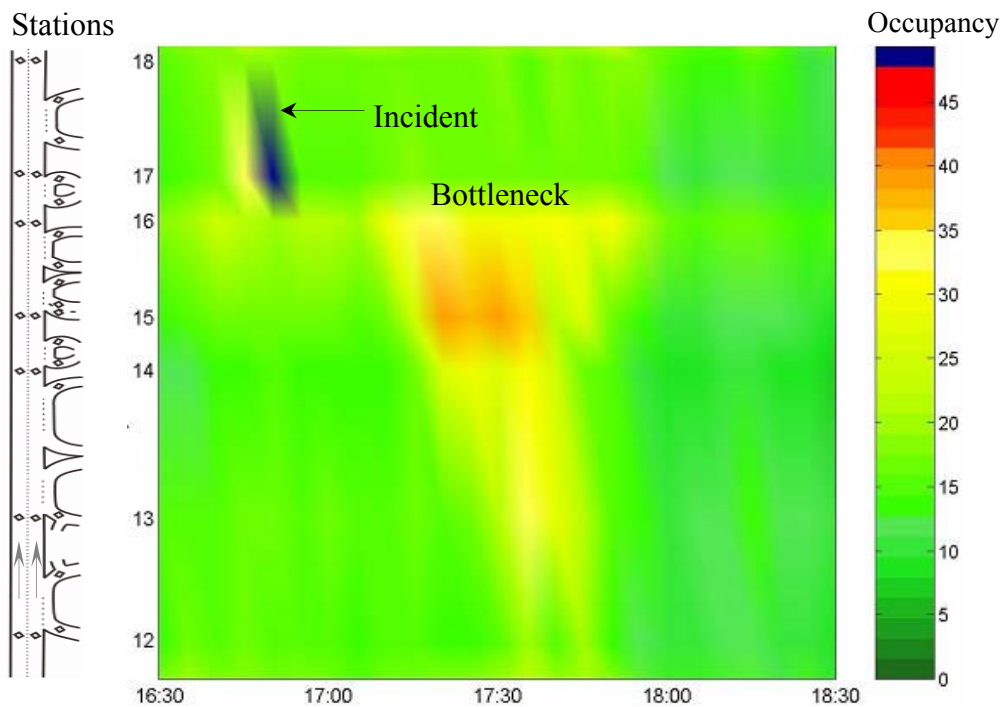


Figure 11: Day One: Occupancy Contour Map

4.1.1 Day One: Bottleneck and Queue Detection

Figure 12 presents oblique curves of cumulative count, N , versus time, t , measured at detector stations 12 to 18. The oblique $N(x, t)$ include counts summed across both lanes at each station. They were constructed by taking linear interpolations through each 30-second count so that their slopes are the flows past the particular detector over each measurement interval. For each station pair, these transformed $N(x, t)$ began with the passage of a reference vehicle so that each curve describes the same collection of vehicles. For each pair of curves, the upstream curve was shifted horizontally to the right by the average free flow trip time from its respective downstream station. Also, for each pair of $N(x, t)$ shown in Figure 12, the upstream curve includes adjusted off-ramp volumes as discussed in section 3. The rescaling rate q_o remained constant for each pair of neighboring stations being compared and therefore did not affect the vertical separations (Cassidy and Windover, 1995).

As seen in Figure 12, the $N(x, t)$ for stations 17 and 18 remain nearly superimposed indicating that the traffic remained freely flowing between these two locations. Flow reductions at the two stations were noticed at 17:17:30 and 17:18:00 respectively. Figure 12 also shows excess vehicle accumulation between stations 16 (adjusted) and 17 around the same time (17:17:30). Evidence from the nearly superimposed $N(x, t)$ between stations 17 (adjusted) and 18 and the excess accumulation between stations 16 (adjusted) and 17 indicate that the bottleneck was located between stations 16 and 17. As shown in Figure 12, a divergence of the curve at station 16 from the one at station 15 (adjusted) is visible at approximately 17:17:00. This time marked the arrival of a backward-moving queue at station 16. There was a pronounced flow reduction at station 16 that accompanied this divergence. This was confirmed by plotting oblique $N(x, t)$ and $T(x, t)$ for station 16 as shown in Figure 13 (a).

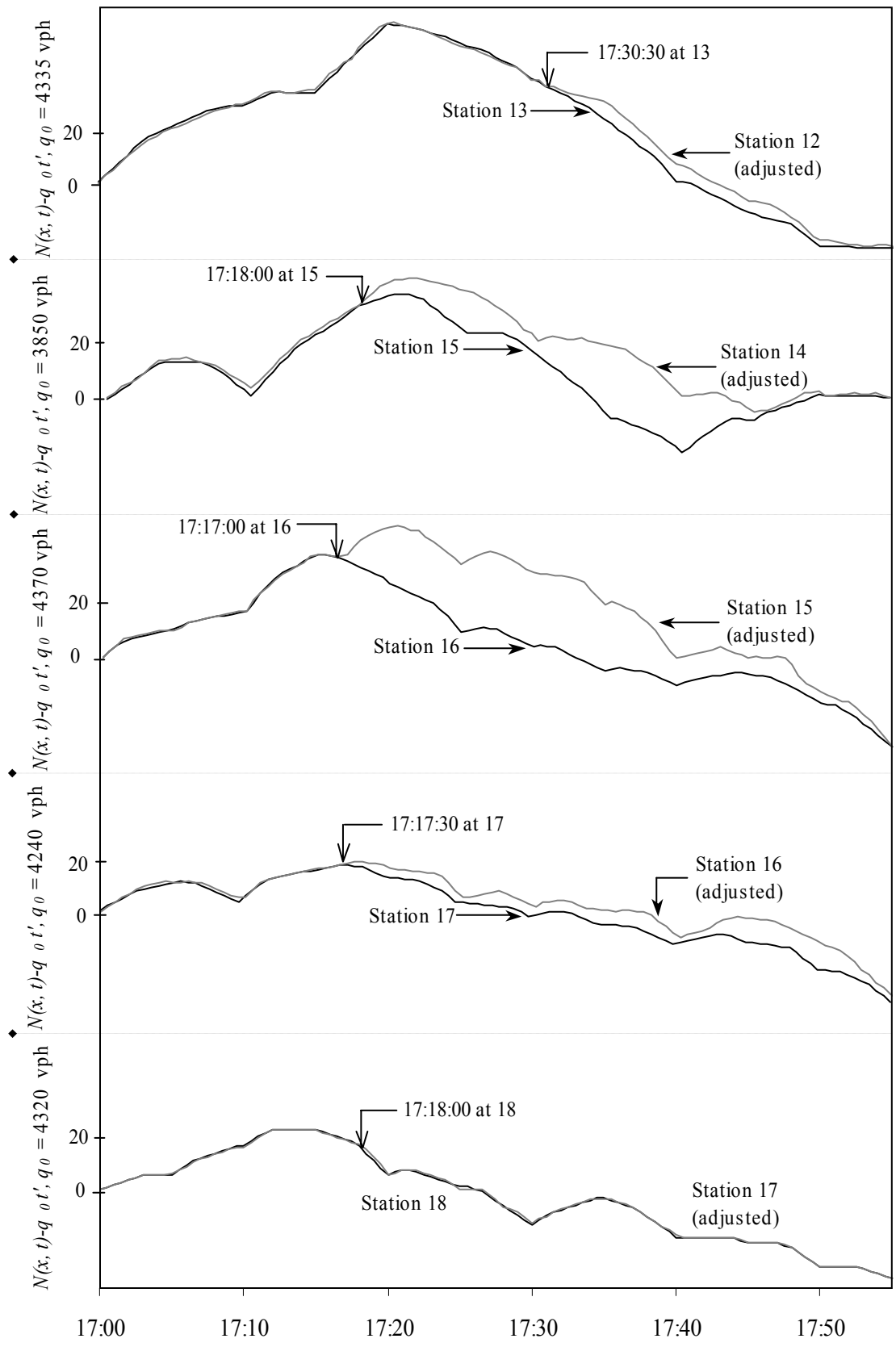


Figure 12: Day One: Transformed $N(x, t)$

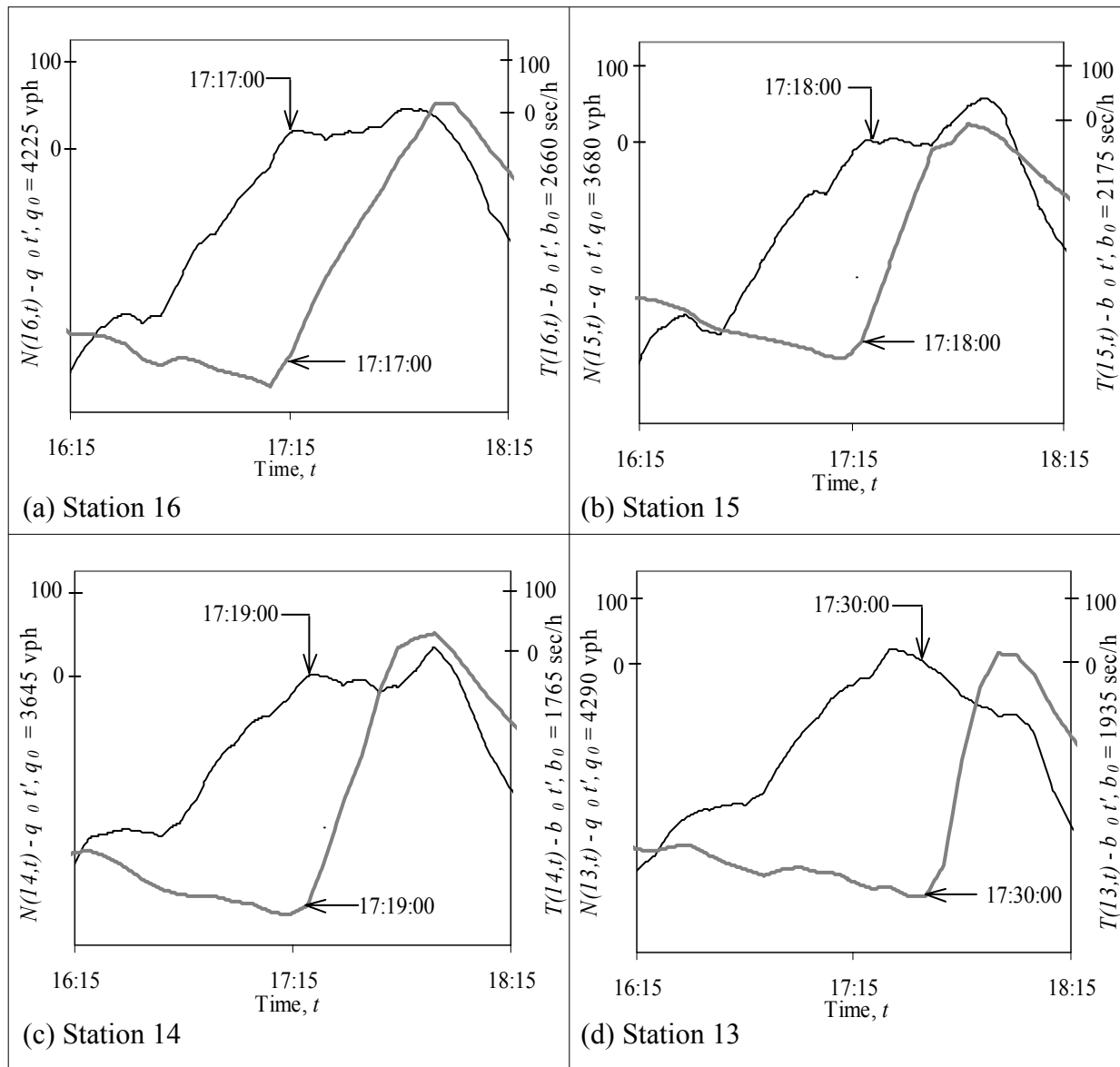


Figure 13: Day One: Oblique $N(x, t)$ and $T(x, t)$

Figure 12 also mapped the propagation of queue upstream of station 16. As shown in the figure, the tail of the queue arrived at station 15 at 17:18:00 (corroborated by the increase in occupancy shown in Figure 13 (b)). Since the ramp counts were not available for the 16th St. on- and off-ramps between stations 13 and 14, the excess accumulation of vehicles between the

two stations could not be traced. However, Figure 13 (c) shows that the queue arrived at station 14 around 17:19:00, marked by a reduction in flow and a simultaneous increase in occupancy.

The backward-moving queue reached station 13 around 17:30:00. Until this time, the nearly superimposed $N(x, t)$ for stations 12 and 13 show that the traffic had been flowing freely between them (Figure 12). This was corroborated by Figure 13 (d) which shows an increase in the oblique $T(x, t)$ at 17:30:00.

In order to understand the traffic flows in each lane, $N(x, t)$ and $T(x, t)$ were constructed for each lane as shown in Figure 14. Note that the backward-moving shock arrived at slightly different times in each lane. To improve the resolution of $N(x, t)$ and $T(x, t)$ in Figure 14, higher rescaling rates were adopted for shoulder lane since flows in this lane were higher than the median lane for all stations.

The time during which the bottleneck remained active was also determined. Figure 15 shows transformed $N(x, t)$ for station 12 (adjusted) and station 18. Station 12 was adjusted to account for the total net inflow of all on- and off-ramps between stations 12 and 18. Figure 15 also shows station 12 without flow adjustments. Between 17:00 and 18:03, an adjustment of 115 vehicles was required to account for conserved net inflow in the section. Thus, correction to flow at station 12 also accounted for the 16th St. interchange between stations 13 and 14 that did not have count data available. In Figure 15, the continued vertical displacement between the two curves shows that the queue persisted until around 18:00:30 when the $N(x, t)$ again became superimposed. After this time, vehicles were traveling in free-flow conditions between these stations. The two insets in Figure 15 show the oblique $N(x, t)$ and $T(x, t)$ curves

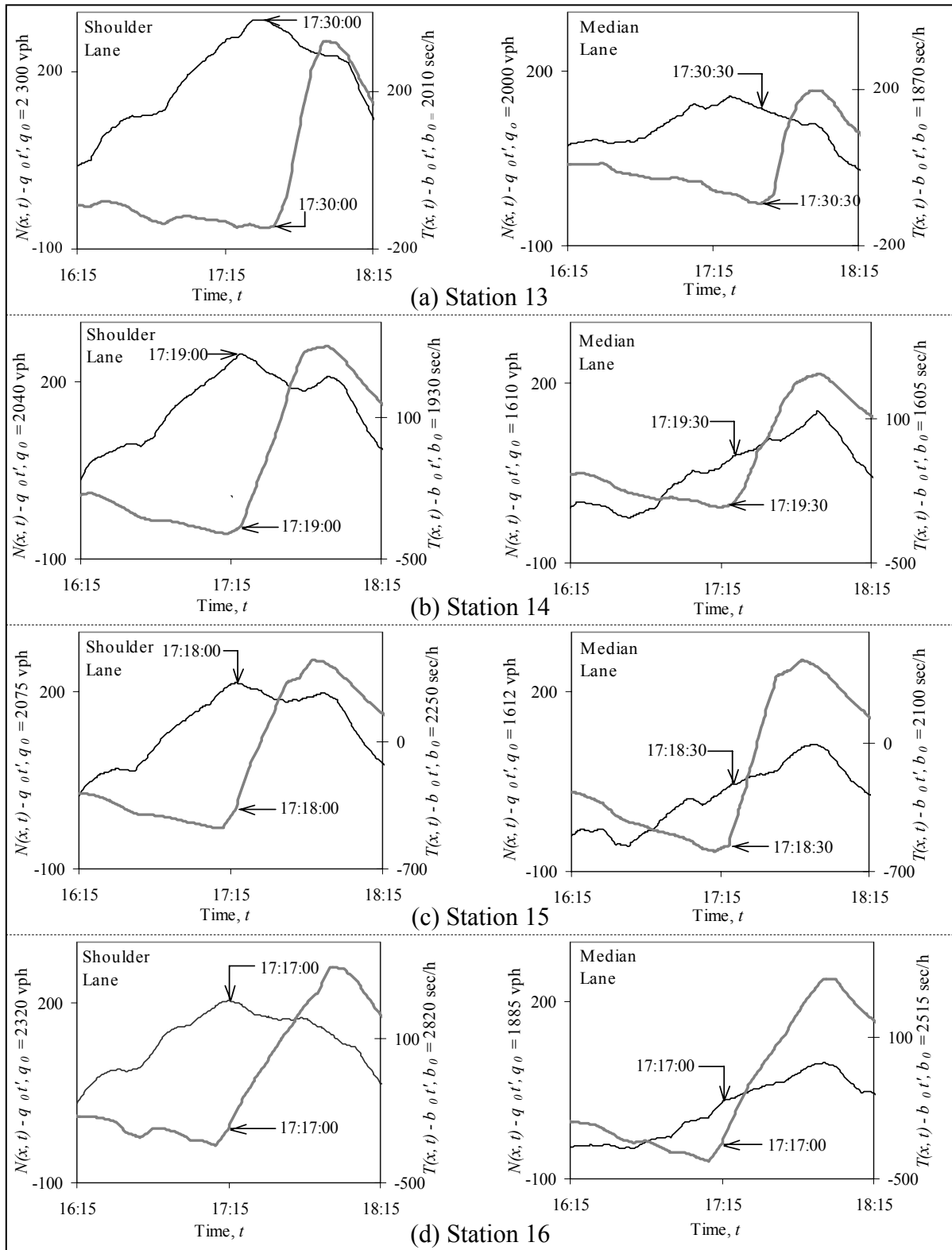


Figure 14: Day One: Oblique $N(x, t)$ and $T(x, t)$ Per Lane (a) Station 13; (b) Station 14; (c) Station 15; (d) Station 16

for stations 12 and 18. At 17:51:00 a reduction in flow and occupancy is visible at station 12 indicating an end of queuing here. Traffic between stations 12 and 18 became freely flowing after 18:00:30.

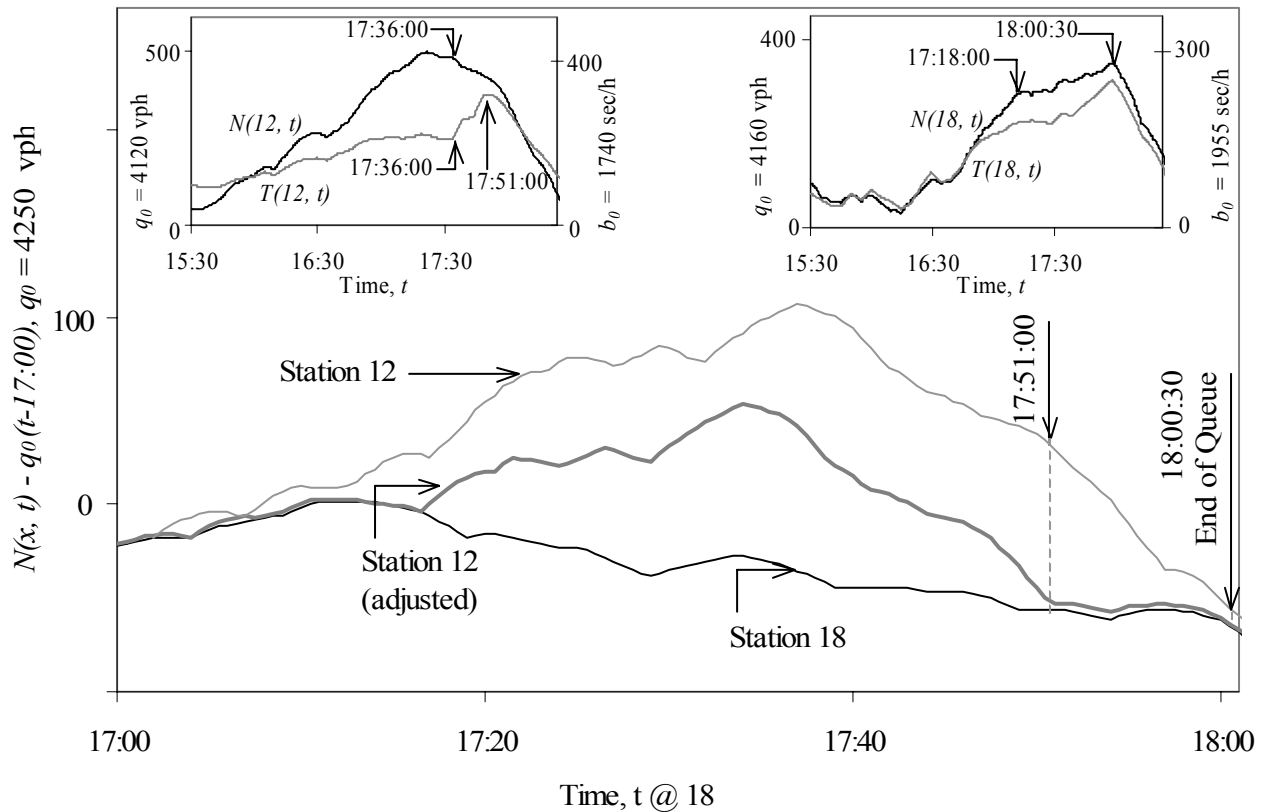


Figure 15: Day One: Transformed $N(x, t)$ Showing End of Queue Between Stations 12 and 18

Figures 11 to 15 have verified the location and time of the bottleneck activation. The queue's propagation was traced over five upstream stations spread over a distance of 2.3 miles (3.7 km). The analyses showed that the bottleneck remained active for almost 43 minutes. The active bottleneck's queue discharge features could now be examined in detail.

4.1.2 Day One: Bottleneck Discharge Flows

To study the discharge flows while the bottleneck was active, oblique $N(x, t)$ and $T(x, t)$ were constructed across both travel lanes at station 18 (downstream of the bottleneck). These are shown in Figure 16. The time interval, spanning about 2.5 hours, includes the period before bottleneck activation, the time it remained active and a later time after it was deactivated. The curves reveal that the traffic conditions at this location were not influenced by any downstream effects; i.e., the curves do not display any abrupt reduction in $N(x, t)$ accompanied by a rise in $T(x, t)$, a feature that would mark the arrival of a queue from downstream. Both curves display very similar features between 17:18:00 and 18:00:30, indicating that discharging vehicles exhibited sequences of nearly stationary traffic patterns with time dependent flows. The intervals delineated by vertical arrows in Figure 16 are periods when the oblique $N(x, t)$ and $T(x, t)$ exhibited small deviations from linear approximations superimposed on these curves (shown with dashed lines). Each of these intervals was characterized by nearly constant flow and nearly uniform vehicle occupancy, shown in units of vehicles per hour and seconds per hour respectively along the dashed lines.

The flow features displayed in Figure 16 show that between 16:15:00 and 18:30:00, station 18 experienced the highest mean flow just before the queue discharge at 17:18:00; about 4475 vph. Soon after, the flow dropped to 4155 vph for about 12 minutes which was a 7% flow reduction. This was followed by a discharge flow of 4285 vph for about 30 minutes. The mean queue discharge flow measured between 17:18:00, the time when queue discharge began, and 18:00:30, when the queue dissipated was 4250 vph. This represented a 5% reduction in flow from that measured prior to queue formation.

Having determined the bottleneck activation time and examined some of its discharge features, we could now analyze its correlation with changes in ramp flows.

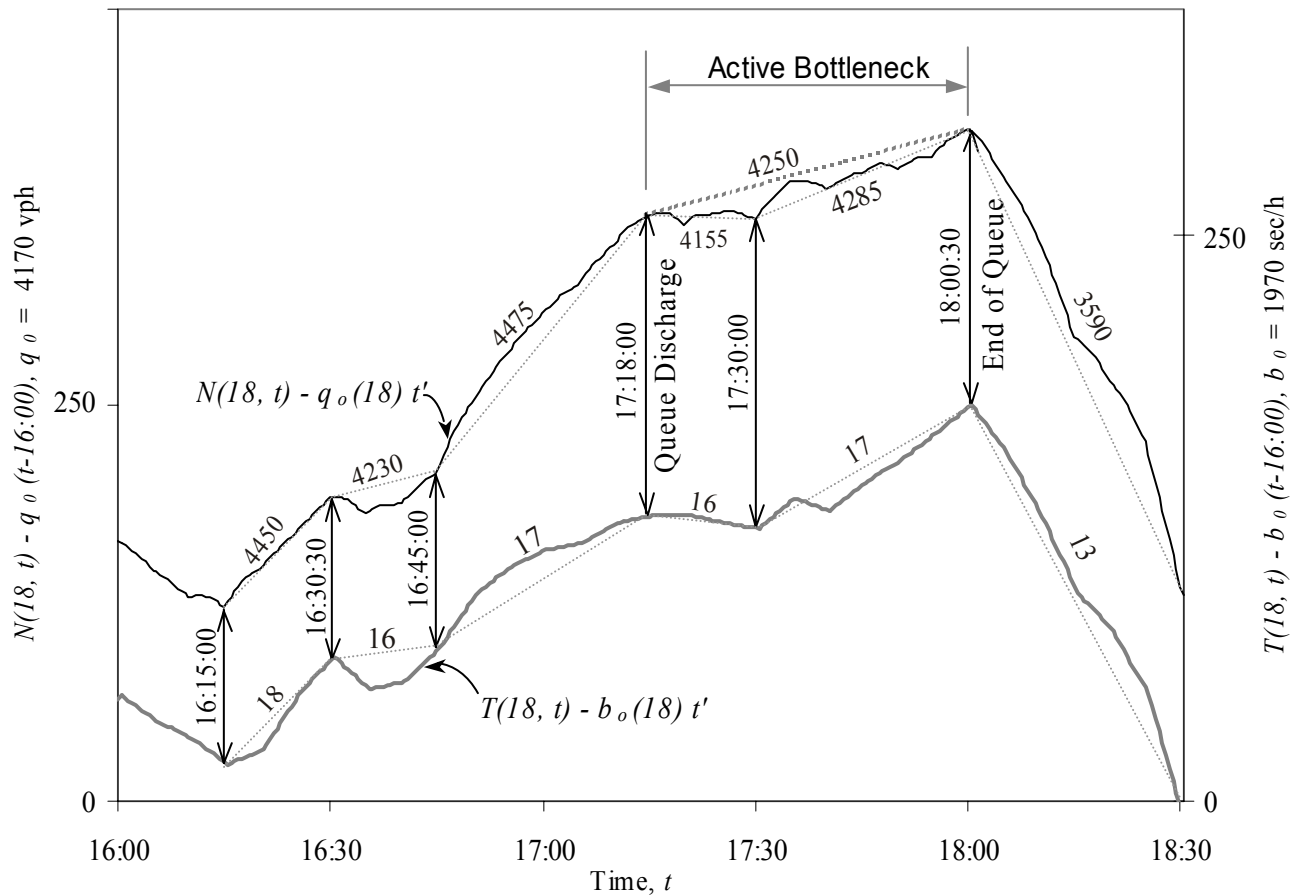


Figure 16: Day One: Oblique $N(x, t)$ and $T(x, t)$ at Station 18

4.1.3 Day One: Ramps Analyses

The on-ramp from TH-55 eastbound (EB) to US 169 is located 370 feet (113 m) downstream of station 16. This is followed by an off-ramp to TH-55 westbound (WB) at a distance of 580 feet (180 m) from the on-ramp. Figure 17 shows oblique $N(x, t)$ for both ramps and Figure 18 is an aerial photo of the interchange. In Figure 17, a sequence of nearly stationary flows was observed and is superimposed on the $N(x, t)$ in units of vph. It appears that

the bottleneck activation time (17:17:30) was preceded by a surge on the off-ramp (at 17:05:00) followed by a surge on the on-ramp (at 17:10:00) that lasted for 7 min. Vehicles were entering the freeway at a low rate of 130 vph for about 12 minutes prior to 17:10:00. This was followed by an increased flow of 240 vph (~ 85% increase) until 17:17:30. Comparing the off-ramp flows to these observations, there was a flow reduction from 320 vph to 200 vph (~ 40% decrease) at 17:17:30. Vehicles entering at 17:17:30 had to merge with the freeway traffic over

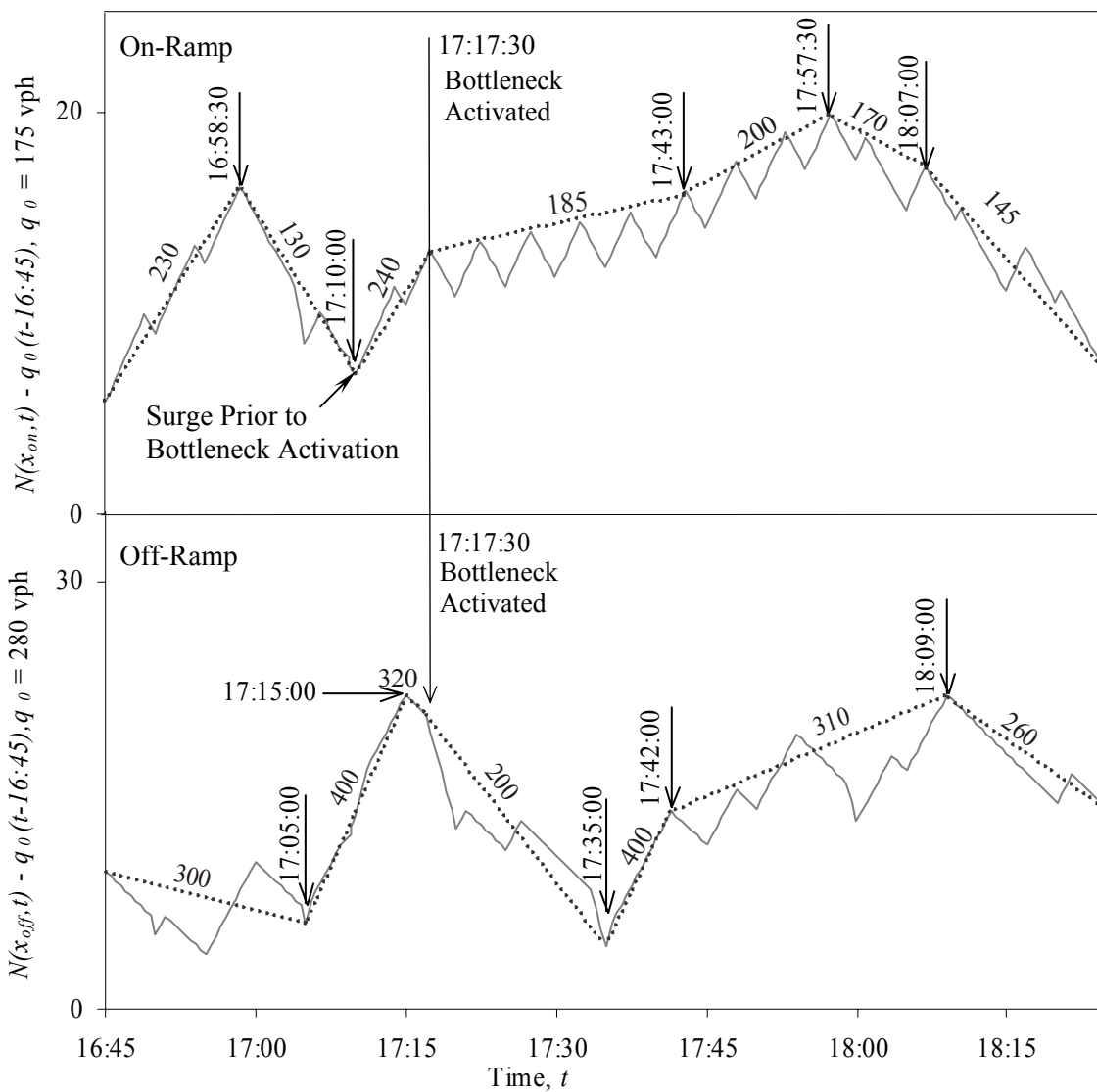


Figure 17: Oblique $N(x, t)$ Showing Ramp Flows Between Stations 16 and 17

a short distance (580 feet or 180 m) by which time there must have been diverging vehicles in the shoulder lane. The lane changing evidently became disruptive, such that periodic slow-downs resulted. The slow-down also led to the apparent restriction of exiting traffic at approximately 17:17:30. Note that this analysis would have benefited if further disaggregate data were available.

From Figure 17, it is clear that the bottleneck arose due to the conflict between merging and diverging traffic just downstream of station 16. Figure 14 (d) shows that the flows in the shoulder lane during these times were higher than the flows in the median lane for station 16. The coincidence of the rise in off-ramp flow, the rise in on-ramp flow, and the apparent restriction in the off-ramp flow for the same time period seemed to trigger the bottleneck. This was also observed for three other days analyzed. For all days, the same merge/diverge conflict seemed to lead to sustained freeway queuing.

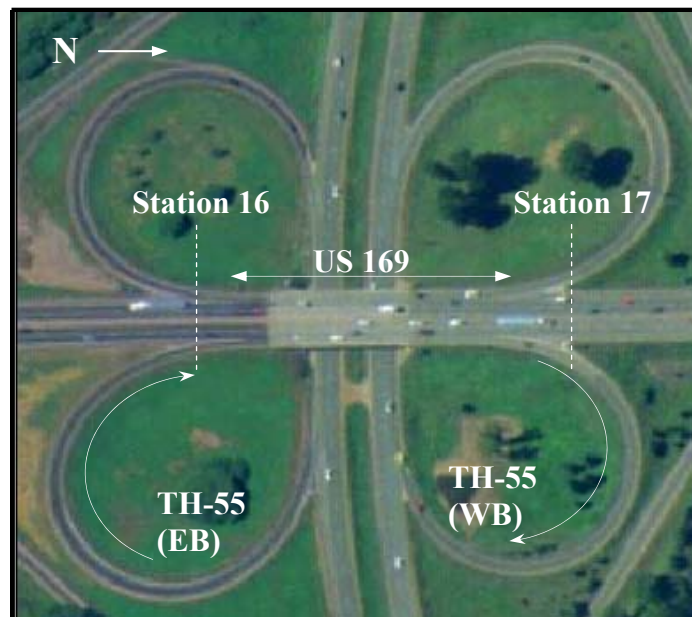


Figure 18: Aerial Photo of US 169 and TH-55 Interchange

The on-ramp flows at all interchanges on all days were metered. On-ramp flows appeared in sequences of peaks and valleys as shown in Figure 17.

4.1.4 Day One: Shock Characteristics

The activation of the bottleneck between stations 16 and 17 was marked by upstream and downstream propagating waves of lower flow. The backward-moving shock marked the arrival of queue at each upstream station. The velocity at which the shock propagated (measured using 30-second data) varied slightly between stations. Table 2 presents the shock characteristics recorded upon bottleneck activation. Note that the wave between stations 17 and 18 was a downstream moving expansion wave of lower flow and lower occupancy. Further analysis showed that these wave velocities could be replicated for other days as well.

Table 2: Shock Velocity Variations

Stations	Section Length		Mean Travel Time Min:sec	Velocity	
	Miles	km		Mi/h	km/h
13-12	0.61	0.98	6:00	- 6	- 10
14-13	0.75	1.20	11:00	- 4	- 7
15-14	0.25	0.40	1:00	-15	- 24
16-15	0.44	0.70	1:00	- 26	- 42
17-18	0.63	1.01	0:30	+ 76	+ 121

The findings in Table 2 are similar to the results of Windover (1998) and Bertini and Leal (2003) who observed that forward- and backward-moving waves have similar velocities. The shock velocity variations observed in Windover (1998) ranged from -6 mph (-10 km/h) to -14 mph (-22 km/h) and those in Bertini and Leal (2003) ranged from -4 mph (-6 km/h) to -8 mph (-13 km/h). As seen in Table 2, the shock velocity variation between stations 12 to 16 is between -4 and -26 mph and is slightly higher than what was observed by the earlier studies.

Those earlier studies benefited from the use of loop detection recorded at a resolution of 1 second. Shock velocities can also vary with driver characteristics of an area. The research to further quantify the relationship between them is still on-going.

4.1.5 Day One: Traffic Oscillations

Queues are characterized by slow-and-go driving conditions, whereby traffic may not come to a complete halt, but drivers experience recurring periods of fast and slow travel (Mauch, 2002). These conditions give rise to start-stop waves that propagate against the flow of traffic and can be seen as sharp increases in flow followed by sudden reductions. Figure 19 shows oscillations observed during 43 minutes of congested traffic by using oblique $N(x, t)$ for six stations; one upstream and five downstream of the bottleneck. The vertical spacing between the curves has been adjusted based on detector distance to enhance clarity. The rescaling rate (q_o) for each $N(x, t)$ equaled the prevailing average 10-minute flow. Hence, the y -axis is $N(t) - \{N[t + 5 \text{ min}] + N[t - 5 \text{ min}]\}/2$; shown as $N - N_{10}$ in the figure. Also, the flows shown in the figure are deviations from average flows (Mauch and Cassidy, 2002).

Figure 19 shows that with the exception of some minor stochastic fluctuations, flows downstream of the bottleneck were fairly steady. Flow oscillations are characteristic of congested traffic and are evident upstream of the bottleneck. The fluctuations noticed on some of the deviation curves are the start-stop waves themselves. As seen in the figure, these waves were characterized by sequences of high and low flows with periods of several minutes each. The amplitudes of each oscillation ($N - N_{10}$) were no more than 40 vehicles across both travel lanes and a scale is provided in Figure 19 to verify this.

Figure 19 also shows that the oscillations' amplitude did not increase steadily in the upstream direction from the bottleneck. Also, visual inspection of the curves in the figure at

any location reaffirms the findings from previous studies (Mauch and Cassidy, 2002) that start-stop waves did not grow systematically over time.

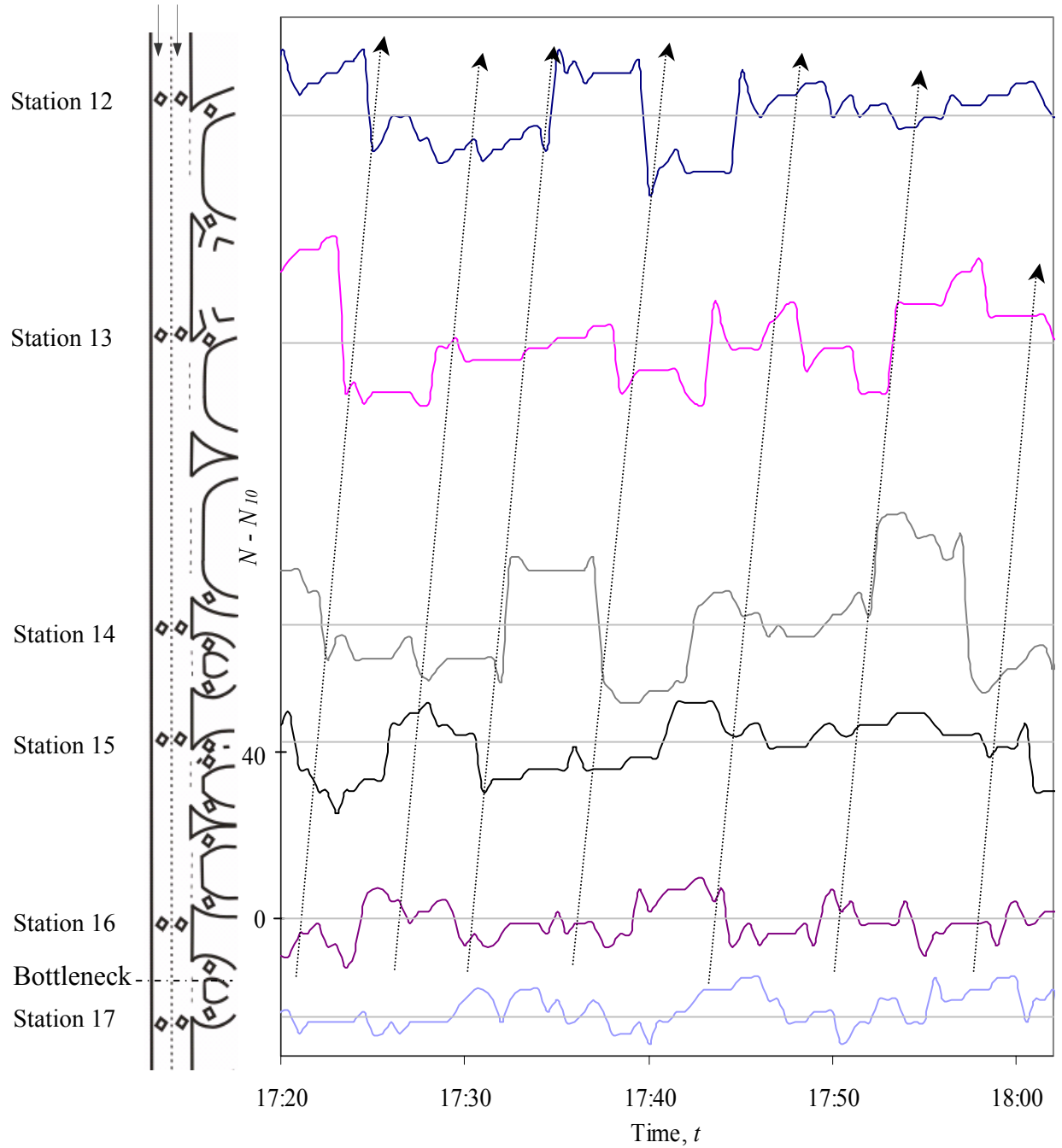


Figure 19: Day One: Deviations from the Prevailing Flows ($N - N_{10}$)

The peaks connected by dashed lines show the paths of the backward-moving oscillations. New waves arose and propagated upstream along with, and parallel to, existing waves. In Figure 19, the dashed lines are nearly parallel to one another. Since the y -axis is representative of the distance between the stations' the slope of the dashed lines is the speed at which the oscillations propagated (Mauch and Cassidy, 2002). As seen in the figure, the oscillations traveled with nearly constant speeds of about 35 to 40 mph (56 to 64 km/hr) and the speed was independent of the location within the queue. Previous studies (Bertini and Leal, 2003; Mauch and Cassidy, 2002) have found lower oscillation speeds ranging between 11 and 15 mph (18 to 24 km/h).

4.2 Reproducing The Observations

The analyses described in the previous sections were repeated for three upstream and two downstream stations from the bottleneck using three additional days of data from US 169. The data were examined for reproducible features. It was revealed that on all four days, the bottleneck arose between stations 16 and 17. On each day, the bottleneck activation time coincided with surge from the on-ramp located between stations 16 and 17. At the same time, the off-ramp just downstream of the on-ramp, exhibited a reduction in flow. Figure 20 shows oblique $N(x, t)$ for the third day (March 22, 2000) for the two ramps located between stations 16 and 17. On this day the bottleneck became active at 16:19:30 and coincided with the on-ramp flow increase.

A detailed analysis of the queue propagation upstream and downstream of the bottleneck for all days is provided in Appendix B. The similarities and variations in flow and queue characteristics on the four days analyzed will be discussed in the following sections.

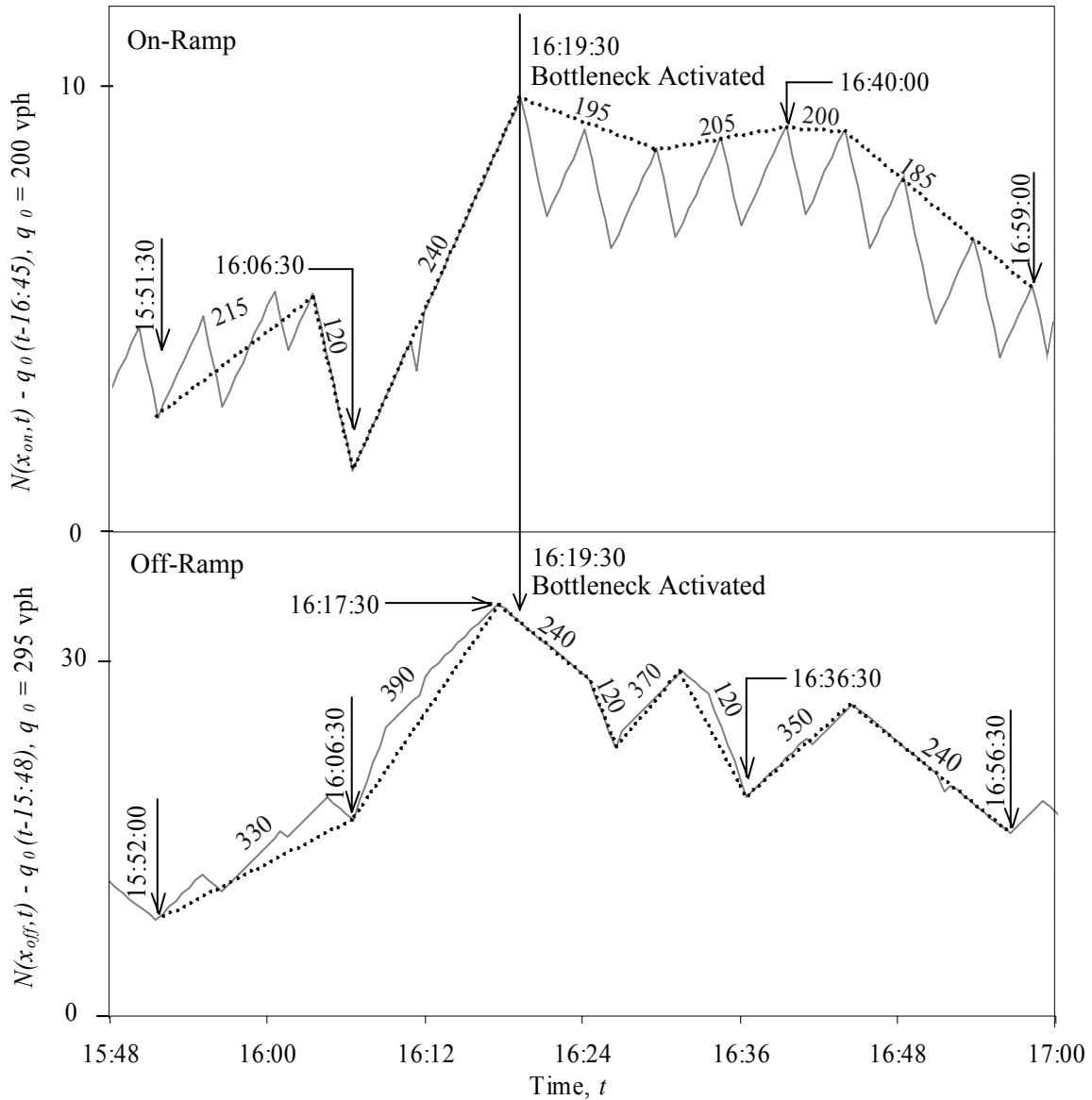


Figure 20: Oblique $N(x, t)$ Showing Ramp Flows Between Stations 16 and 17 (Day Three)

4.2.1 Reproducible Bottleneck Features

Reproducible bottleneck features are summarized in Table 3. The table shows the flows immediately prior to upstream queue formation and the average discharge rates that prevailed while bottleneck was active. The durations of high flows prior to queuing were relatively short. The flows during these times and the durations varied somewhat from day to day. The

magnitudes and durations of the discharge flows that followed the onset of queuing were quite consistent with a mean rate of 4260 vph. This finding is consistent with what was observed in earlier studies (e.g. Bertini and Cassidy, 2002; Cassidy and Bertini, 1999a; Cassidy and Bertini, 1999b) that showed possible instabilities in both durations and flows prior to queuing and consistent discharge flow after the onset of queuing. Bertini and Leal (2003) also found that flows before queue formation could have consistent characteristics.

Table 3 also shows that the mean flow prior to queue discharge was 4450 vph. The flow reduction measured upon queue formation was also reproducible from day to day, ranging from 2 to 5%.

Table 3: Summary of Measured Traffic Features

Day	Date	Flow Immediately Prior to Queue		Average Discharge Rate		Percent Drop (a)-(b) %
		Rate (a) vph	Duration h:min:sec	Rate (b) vph	Duration h:min:sec	
Monday	20-Mar-2000	4475	0:32:30	4250	0:42:00	5
Tuesday	21-Mar-2000	4440	0:19:00	4230	0:51:00	5
Wednesday	22-Mar-2002	4340	0:10:00	4260	0:25:00	2
Thursday	23-Mar-2000	4530	0:19:30	4290	0:19:30	5
Mean		4450		4260		4
Standard Deviation		80		25		

4.2.2 Variation in Shock Propagations

The shocks that marked the onset of queuing were analyzed for the additional 3 days. The results for four days were averaged and are shown in Table 4. The backward-moving shock traveled with velocities ranging from 20 to 24 mph. There were only slight differences between the times shocks took to propagate between stations from day to day. The forward-moving

waves showed a mean velocity of 76 mph. Due to the arbitrary aggregation at a 30-second level, it was difficult to pinpoint velocities, especially for the forward-moving waves.

Table 4: Four Days - Shock Characteristics

Stations	Mean of 4 Days				
	Section Length		Mean Travel Time	Velocity	
	Miles	km		Min:sec	Mi/h
15-14	0.25	0.40	0:45	-20	-32
16-15	0.44	0.70	1:08	-24	-38
17-18	0.63	1.01	0:30	+76	+121

5. CONCLUSIONS

An active bottleneck arose whenever flows from an upstream on-ramp reached a certain peak. The location of the bottleneck was consistent from day to day, between an on-ramp and a downstream off-ramp located between stations 16 and 17. This conclusion follows from observation that the bottleneck activation time always coincided with the surges from the on-ramp, accompanied by an apparent flow restriction on the off-ramp. After the bottleneck became active, the queue propagated to both freeway lanes. A sudden drop in flow accompanied by a rise in occupancy marked the arrival of queue at each successive upstream station. The onset of congestion sent forward- and backward-moving waves that had nearly constant velocities for all days analyzed. The bottleneck activation had marked effects on its discharge flows. Average queue discharge rates were approximately 2 to 5% lower than the flows that prevailed prior to the bottleneck's activation. It was also observed that these discharge flows in active bottlenecks exhibited near stationary patterns about a nearly constant rate. The bottleneck's long-run discharge rates were consistent from day to day. The analysis also showed that waves in congested traffic traveled with reproducible velocities. Additionally,

the oscillations that arose in queued traffic appeared only at upstream stations. The oscillations' effects did not grow steadily in amplitudes while propagating upstream of bottleneck's location.

It follows that bottlenecks that arise at fixed reproducible locations can be predicted. As a remedy to recurring bottlenecks that result due to ramp flows, suitable metering techniques should be investigated that consider the mainline flows. In this study no attempt was made to assess the impact of metering rates used by the Mn/DOT on bottleneck activation. An earlier study (Cassidy and Rudjanakanoknad, 2002) of the role of ramp metering for averting bottlenecks on freeways noted that service rates at such sites could be increased: 1) by eliminating or postponing the bottleneck's activation; and 2) by mitigating downstream slow-downs if and when the activation occurred. It further showed that these objectives could be realized by carefully metering an on-ramp to limit the rates at which its vehicles joined the freeway traffic stream. The idea should be to increase flows at locations where a queue would have otherwise impeded traffic, particularly if the queue was kept from propagating past busy off-ramps and starving them of flows. This observation is also true for the site examined on US 169.

These findings, while important in their own right, remain consistent with what has been observed elsewhere in literature at sites in Canada and the U.K. The study was unique in that it confirmed these results for a freeway in the U.S. and showed that traffic behaved as if passing over links where on- and off-ramps existed. Further experiments will be required that can test the effects of metering rates for postponing (or perhaps eliminating) the bottleneck's activation. This study used data from a freeway in Minnesota before its DOT had conducted the ramp meter shut-off experiment. Future research aimed at measuring the benefits of intelligent

transportation system (ITS) could study traffic behavior for days when ramp meters had been turned off.

Also, the extent to which driver behavior can be related to flow characteristics, shock speeds and oscillations' propagation are areas that need further investigation. With additional research in this area, benefits can be reaped by the application of these theories that can predict a bottleneck and queue discharge rates. Research should cover several other sites in U.S., Europe and Asia and consider various road geometrics to confirm the application of theories used herein. Finally, confident results based on extensive empirical evidence will encourage highway managers to use this information for easing congestion and for the placement of ITS related devices to aid in traveler information and increasing safety.

REFERENCES

- Bertini, R.L. (1999). *Time Dependent Traffic Flow Features at a Freeway Bottleneck Downstream of a Merge*. Ph.D. Thesis, University of California, Berkeley, U.S.A.
- Bertini, R.L. and Cassidy, M.J. (2002). Some Observed Queue Discharge Features at a Freeway Bottleneck Downstream of a Merge. *Transportation Research*, Vol. 36A, pp. 683-697.
- Bertini, R.L. and Leal, M. (2003). Empirical Study of Traffic Features at a Freeway Lane Drop. *Transportation Research*, Part A, Policy and Practice, Elsevier (Submitted).
- Cassidy, M.J. (1998). Bivariate Relations in Nearly Stationary Highway Traffic. *Transportation Research*, Vol. 32B, pp. 49-59.
- Cassidy, M.J., Anani, S.B. and Haigwood J.M. (2002). Study of Freeway Traffic Near an Off-Ramp. *Transportation Research*, Vol. 36A, pp. 563-572.
- Cassidy, M.J. and Bertini, R.L. (1999a). Some Traffic Features at Freeway Bottlenecks. *Transportation Research*, Vol. 33B, pp. 25-42.
- Cassidy, M.J. and Bertini, R.L. (1999b). Observations at a Freeway Bottleneck. *Proceedings of the Fourteenth International Symposium on Transportation and Traffic Theory*, Jerusalem, Israel, pp. 107-124.
- Cassidy, M.J. and Mauch, M. (2001). An Observed Traffic Pattern in Long Freeway Queues. *Transportation Research*, Vol. 35A, pp. 143-156.
- Cassidy, M.J. and Rudjanakanoknad J. (2002). *Study of Traffic at a Freeway Merge and Roles for Ramp Metering*. California PATH Working Paper UCB-ITS-PWP-2002-2. Institute of Transportation Studies, University of California, Berkeley, U.S.A.
- Cassidy, M.J. and Windover J.R. (1995). Methodology for Assessing Dynamics of Freeway Traffic Flow. *Transportation Research Record 1484*, TRB, National Research Council, Washington, D.C., pp. 73-79.
- Daganzo, C.F. (1997). *Fundamentals of Transportation and Traffic Operations*. Elsevier, New York.
- Lawson, T.W., Lovell, D.J., and Daganzo, C.F. (1997). Using Input-Output Diagram to Determine Spatial and Temporal Extents of a Queue Upstream of a Bottleneck. *Transportation Research Record 1572*, TRB, National Research Council, Washington, D.C., pp. 140-147.
- Mauch, M. (2002). *Analysis of Stop-Start Waves in Congested Freeway Traffic*. Ph.D. Thesis, University of California, Berkeley, U.S.A.

- Mauch, M. and Cassidy, M.J. (2002). Freeway Traffic Oscillations: Observations and Predictions. *Proceedings of the Fifteenth International Symposium on Transportation and Traffic Theory*, Adelaide, Australia, pp. 653-673.
- May, A.D. (1990). *Traffic Flow Fundamentals*. Prentice Hall, Englewood Cliffs, New Jersey.
- Munoz, J.C. and Daganzo, C. F. (2000). *Experimental Characterization of Multi-lane Freeway Traffic Upstream of an Off-Ramp Bottleneck*. California PATH Working Paper UCB-ITS-PWP-2000-13. Institute of Transportation Studies, University of California, Berkeley, U.S.A.
- Newell, G.F. (1993). A Simplified Theory of Kinematic Waves in Highway Traffic; I: General Theory, II: Queuing at Freeway Bottlenecks, III: Multi-destination Flows. *Transportation Research*, Vol. 27B (4), pp. 281-313.
- Windover, J.R. (1998). *Empirical Studies of the Dynamic Features of Freeway Traffic*. Ph.D. Thesis, University of California, Berkeley, U.S.A.
- Windover, J.R. and Cassidy, M.J. (2001). Some Observed Details of Freeway Traffic Evolution. *Transportation Research*, Vol. 35A, pp. 881-894.

APPENDIX A

March, 2000
 Preliminary Local Climatological Data
 Minneapolis/St. Paul, MN
 National Weather Service

Day	Date	Temperature		Precipitation	Snowfall	
		Degree F		Inches	Inches	
	da-mo-yr	Maximum	Minimum	Total	Normal for Month	
Monday	20-Mar-2000	45	36	0	0.72	0
Tuesday	21-Mar-2000	49	40	0	0.72	0
Wednesday	22-Mar-2002	53	43	0	0.72	0
Thursday	23-Mar-2000	64	47	0.19	0.91	0

Weather data shown above was downloaded from the University of Minnesota's website at <http://www.soils.umn.edu/> (Department of Soils, Water and Climate) on May 7, 2003. The data shows that the days were appropriate for the study.

APPENDIX B

Details of Shock Variations by Day

Tables 4 to 7 show the shock characteristics for all four days studied. The shock travel times and hence the velocity varied slightly from day to day between stations. The forward-moving waves recorded much higher velocities.

Table 5: Day 1 - Shock Propagation

20-Mar-2000						
Station	Section Length		Fluctuation Arrival Time	Travel Time	Velocity	
	Miles	km			Min:sec	Mi/h
14			17:19:00			
15	0.25	0.40	17:18:00	1:00	-15	-24
16	0.44	0.70	17:17:00	1:00	-26	-42
18	0.63	1.01	17:18:00	0:30	+76	+121

Table 6: Day 2 - Shock Propagation

21-Mar-2000						
Station	Section Length		Fluctuation Arrival Time	Travel Time	Velocity	
	Miles	km			Min:sec	Mi/h
14			17:15:00			
15	0.25	0.40	17:14:30	0:30	-30	-48
16	0.44	0.70	17:13:00	1:30	-18	-29
18	0.63	1.01	17:14:00	0:30	+76	+121

Table 7: Day 3 - Shock Propagation

22-Mar-2002						
Station	Section Length		Fluctuation Arrival Time	Travel Time	Velocity	
	Miles	km			Min:sec	Mi/h
14			16:21:00			
15	0.25	0.40	16:20:00	1:00	-15	-24
16	0.44	0.70	16:19:00	1:00	-26	-42
18	0.63	1.01	16:20:00	0:30	+76	+121

Table 8: Day 4 - Shock Propagation

23-Mar-2000

Station	Section Length		Fluctuation Arrival Time	Travel Time	Velocity	
	Miles	km			Min:sec	Mi/h
14			17:40:30			
15	0.25	0.40	17:40:00	0:30	-30	-48
16	0.44	0.70	17:39:00	1:00	-26	-42
18	0.63	1.01	17:40:00	0:30	+76	+121